Morey

MINNESOTA GEOLOGICAL SURVEY
INFORMATION CIRCULAR 44

GEOCHEMICAL EVALUATION OF PLATINUM GROUP ELEMENT (PGE) MINERALIZATION IN THE SONJU LAKE INTRUSION, FINLAND, MINNESOTA

UNIVERSITY OF MINNESOTA

MINNESOTA GEOLOGICAL SURVEY
D.L. Southwick, *Director*

Information Circular 44

GEOCHEMICAL EVALUATION OF PLATINUM GROUP ELEMENT (PGE) MINERALIZATION IN THE SONJU LAKE INTRUSION, FINLAND, MINNESOTA

By
James D. Miller, Jr.

UNIVERSITY OF MINNESOTA
St. Paul, 1999

This publication is accessible from the home page of the Minnesota Geological Survey (http://www.geo.umn.edu/mgs) as PDF files readable with Acrobat Reader 4.0.

Date of release, October 22, 1999

Recommended citation:

Miller, J. D., Jr., 1999, Geochemical Evaluation of Platinum Group Element (PGE) Mineralization in the Sonju Lake Intrusion, Finland, Minnesota:
Minnesota Geological Survey Information Circular 44, 31 p.

Minnesota Geological Survey
2642 University Avenue West
Saint Paul, Minnesota 55114-1057

Telephone: 612-627-4780
Fax: 612-627-4778
E-mail address: mgs@tc.umn.edu
Web site: http://www.geo.umn.edu/mgs

ISSN 0544-3105

CONTENTS

FIGURES

TABLES

APPENDIX TABLES

GEOCHEMICAL EVALUATION OF PLATINUM GROUP ELEMENT (PGE) MINERALIZATION IN THE SONJU LAKE INTRUSION, FINLAND, MINNESOTA

James D. Miller, Jr.

SUMMARY

This study was undertaken to evaluate the potential for stratiform platinum group element (PGE) mineralization in the Sonju Lake intrusion (SLI). The SLI is a well-differentiated, tholeiitic, mafic layered intrusion that is part of the multiple intrusive Beaver Bay Complex, and is exposed near Finland, Minnesota. Geochemical analyses of outcrop and drill-core samples that span the 1200-m-thick SLI were interpreted in the context of (1) data from PGE reefs in other tholeiitic layered intrusions (most notably the Skaergaard intrusion of East Greenland), and (2) models of PGE and sulfide mineralization in tholeiitic intrusions. The geochemical data show that a PGE-mineralized horizon is present approximately two-thirds of the way up from the base of the moderately south-dipping, sheet-like SLI. PGE mineralization was apparently related to initial sulfide saturation and subsequent exsolution of sulfide melt from the SLI magma. The data also indicate that as it settled, the sulfide melt efficiently scavenged PGEs from the SLI magma, and concentrated them into a relatively narrow interval of gabbroic cumulates. The geochemical signature of the SLI is remarkably similar to that of the PGE-bearing Platinova reef in the Skaergaard intrusion. The highest Pd, Pt and Au concentrations in SLI outcrop samples are far from economic grade (360, 66, and 85 ppb respectively); but a more precise evaluation of peak grade, thickness, and lateral continuity requires drilling and analysis of the entire interval. When the results of the study reported here are combined with evidence for similar mineralization in the Layered Series at Duluth, they indicate that tholeiitic layered intrusions of the Duluth and Beaver Bay complexes are favorable exploration targets for reef-type PGE mineralization.

BACKGROUND

Economic concentrations of platinum group elements (PGEs) in meter-thick, stratiform, sulfide-bearing horizons (PGE reefs) have long been known to be associated with ultramafic-mafic layered intrusions such as the Bushveld and Stillwater complexes (Naldrett, 1993). Typically, PGE reefs are present near the transition from ultramafic to mafic rocks; they were not previously thought to exist in tholeiitic intrusions, which lack significant volumes of ultramafic rock. However, recent discoveries of stratiform PGE mineralization in the Skaergaard intrusion and related bodies of East Greenland (Bird and others, 1991, 1995; Neilsen and Brooks, 1995; Aranson and others, 1997;

Andersen and others, 1998) show that PGE reefs may also exist in tholeiitic layered intrusions. The presence of many mafic layered intrusions of tholeiitic composition associated with the 1.1 Ga Midcontinent Rift in northeastern Minnesota suggests that it is fertile ground for exploration for this newly recognized type of PGE mineralization.

The Minnesota Geological Survey (MGS), with the support of the Minerals Coordinating Committee (MCC), has been studying the potential for stratiform PGE mineralization in tholeiitic intrusions of northeastern Minnesota since 1993. In the 1993-95 fiscal biennium, funding was received to evaluate the potential for PGE reef mineralization in the Layered Series at Duluth (DLS in Fig. 1). That study showed several anomalously high PGE concentrations associated with sulfide mineralization, and indicated that a favorable horizon might occur in the medial part of the DLS (Miller, 1995, 1998a, 1998b). Those results, although interesting, were not definitive enough

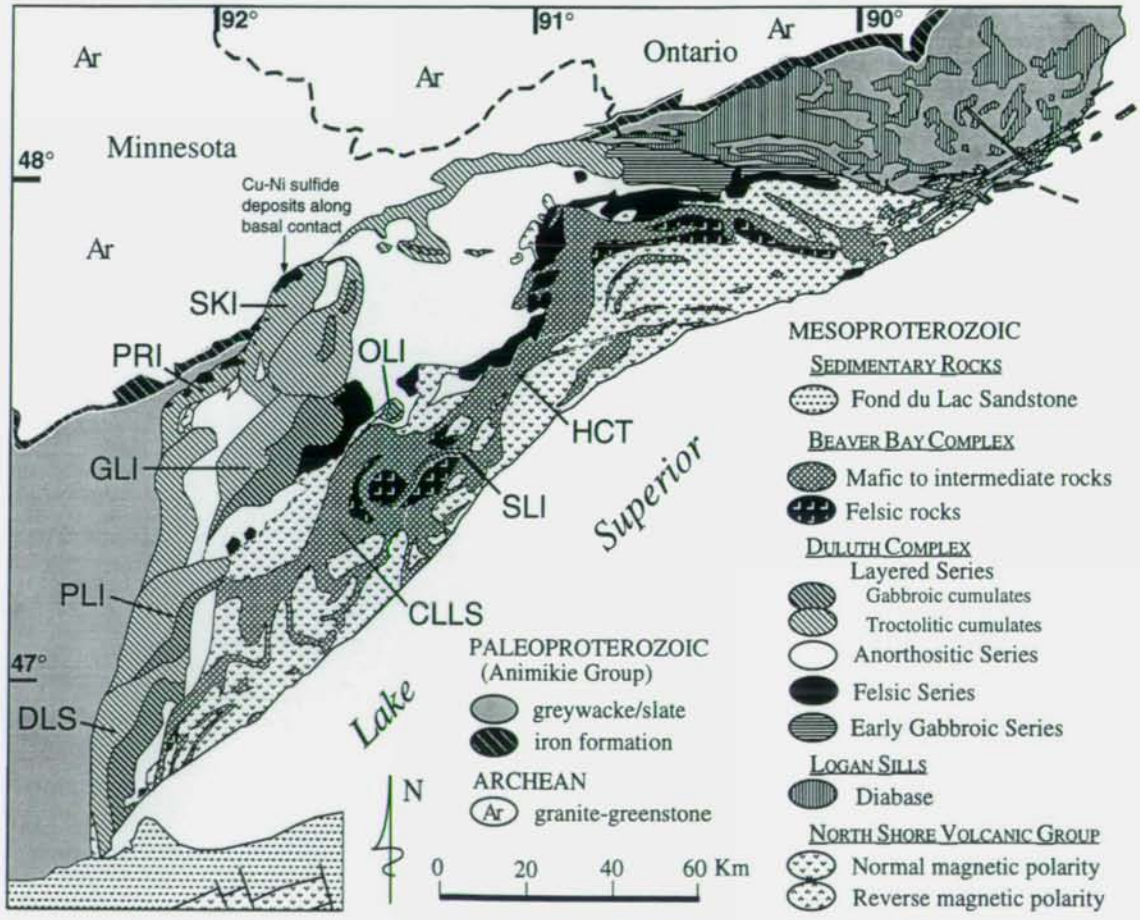

Figure 1. Generalized geology of the Duluth and Beaver Bay complexes and related Proterozoic rocks of northeastern Minnesota. Intrusions discussed in the text are: SLI—Sonju Lake intrusion, DLS—Layered Series at Duluth, PRI—Partidge River intrusion, SKI—South Kawishiwi intrusion, GLI—Greenwood Lake intrusion, OLI—Osier Lake intrusion, PLI—Pequayan Lake intrusion, CLLS—Cloquet Lake layered series, HCT—Houghtaling Creek troctolite macrodike. Black areas along basal contact of PRI and SKI bodies denote Cu-Ni sulfide deposits.

to convince the State or exploration companies to evaluate the PGE potential of the DLS further. The geochemical data were difficult to interpret because the DLS evolved as a fairly complex, open-magmatic system. Research needed to target an intrusion that formed from a simpler, more nearly-closed magma system, similar to the Skaergaard. The Sonju Lake intrusion near Finland (Fig. 1) is such a closed-system intrusion. This past winter (1998/1999) the MGS received supplemental funding from the MCC to conduct a geochemical study of the Sonju Lake intrusion. This report gives the results of that study.

Criteria for Evaluation of Stratiform PGE Potential in Tholeiitic Intrusions

Opinion swings back and forth regarding the relative importance of hydrothermal processes in the concentration of PGEs into stratiform horizons in mafic layered intrusions, but it is generally agreed that primary magmatic processes play a major role (Naldrett, 1993). Because PGEs are strongly chalcophile, most models imply that mafic magma systems have concentrated PGEs by bringing PGE-bearing magmas or fluids into contact with sulfide melts or minerals. Most commonly, this is accomplished when an immiscible sulfide melt separates from a PGE-bearing magma reservoir and settles through the silicate fraction, scavenging PGEs on the way. The degree to which the sulfide melt becomes enriched in PGEs is dependent on PGE abundance in the magma, and especially on the volume of silicate magma encountered by the sulfide melt as it settles to the floor or margins of the magma chamber. Mafic rocks can also be enriched in PGEs by the fluxing of PGE-bearing hydrothermal fluids (mostly Cl-brines) through sulfide-bearing gabbro (Boudreau and McCallum, 1992). Even during hydrothermal enrichment processes, the sulfide that provides the geochemical trap for the PGEs may well have formed magmatically (Barnes and Campbell, 1988). Therefore, evaluation of the potential that a mafic layered intrusion has for hosting stratiform PGE mineralization requires knowledge of the history of sulfide saturation and segregation in the magma system.

Based on empirical observations of PGE mineralization in the Skaergaard and other tholeiitic layered intrusions, as well as on theoretical considerations of S and PGE behavior in differentiating, dynamic intrusions (Naldrett, 1993), the following conditions are understood to favor the formation of PGE-enriched horizons in tholeiitic layered intrusions:

1. The parent magma be initially sulfide undersaturated.
2. The parent magma have a high initial PGE concentration and/or experience a considerable amount of fractional crystallization to build up PGE concentrations prior to sulfide saturation.
3. The initial segregation of sulfide melt be triggered by a process (e.g., magma mixing, decompression, assimilation, simple differentiation) that promotes a high silicate/sulfide melt ratio.

These conditions suggest that the optimal location for significant PGE mineralization in a well-differentiated tholeiitic layered intrusion is at a mid- to upper-level horizon that records the initial saturation of sulfide in the magma. Theoretically, a gabbro cumulate crystallized from a magma saturated in sulfide should contain more than 400 ppm S (Boudreau and McCallum, 1992). Regardless of how sulfide saturation is triggered, or the physical manner in which sulfide melt arrives at the magma chamber floor, it is likely that the first sulfide melt to be segregated has the greatest potential for encountering the most PGE-enriched silicate magma. Thus, exploration for

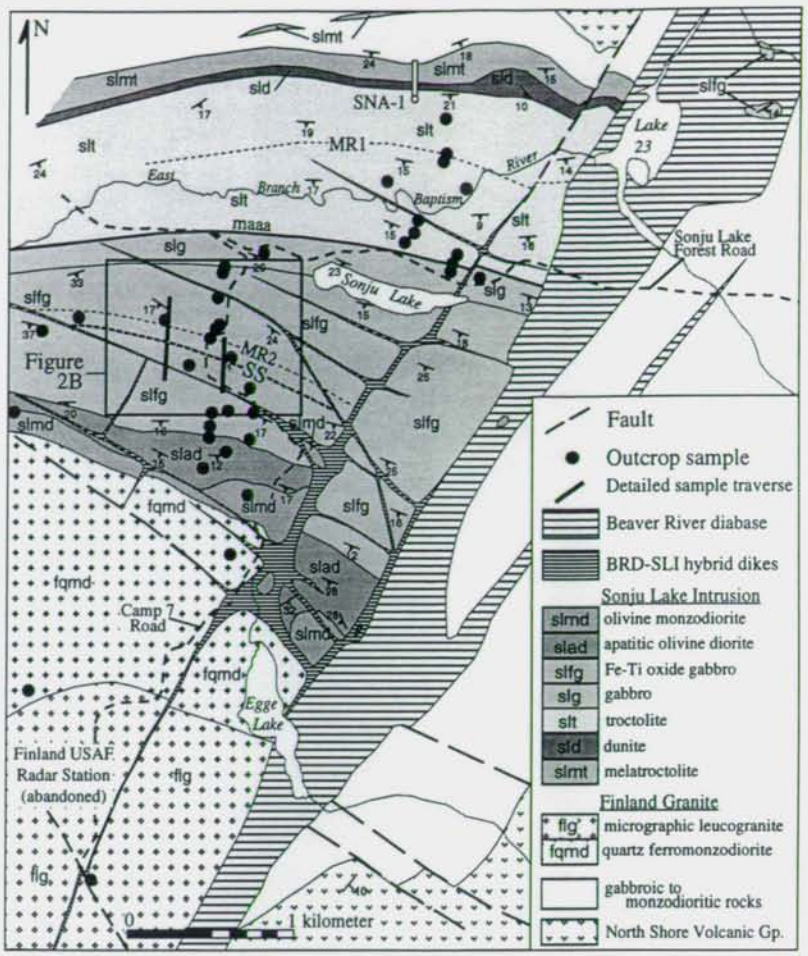

Figure 2A. See page 5 for caption

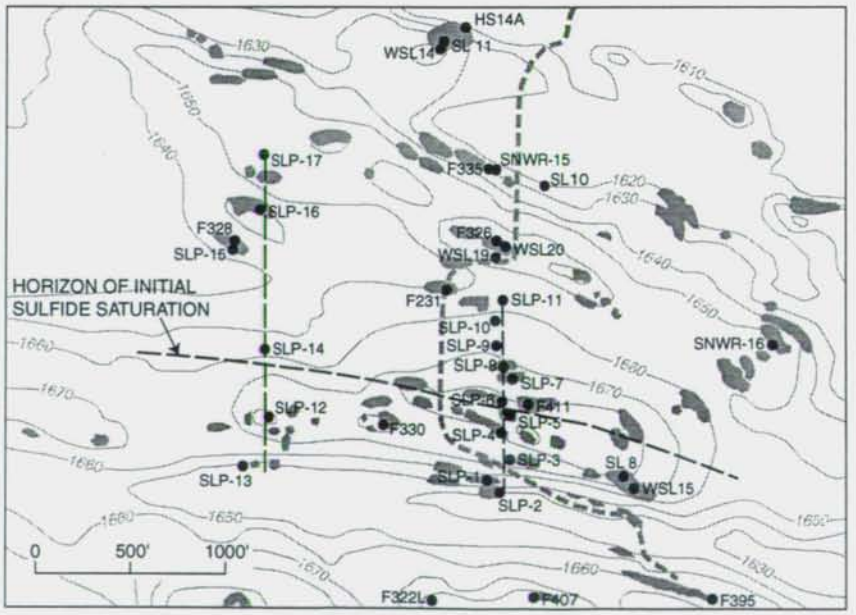

Figure 2B. See page 5 for caption

a PGE-enriched interval should attempt to seek out the stratigraphically lowest gabbroic cumulates that contain 400 ppm or more sulfur. The Cu/Pd ratio also gives an indication of the effectiveness of the sulfide segregation event in scavenging chalcophile metals from the silicate magma. Because Pd is several orders of magnitude more compatible with sulfide melt than Cu, a silicate melt efficiently scavenged of Pd should have an increased Cu/Pd ratio after a sulfide segregation event (Barnes and others, 1993).

Geology of the Sonju Lake Intrusion

The Sonju Lake intrusion (SLI) is a 1200-m-thick tholeiitic mafic layered intrusion that is exposed about 8 km north of Finland, Minnesota. In the 9 km^2 area centered on Sonju Lake where it is exposed, the SLI is composed of a moderately south-dipping, well-differentiated sequence of mafic cumulates (Fig. 2A). The SLI is part of the Beaver Bay Complex, which is a suite of intrusions emplaced into the upper part of the Mesoproterozoic North Shore Volcanic Group (Fig. 1; see also Miller and Chandler, 1997 and 1999). Baddelyite from ferrogabbro in the upper part of the SLI yields a U-Pb age of 1096.1±0.8 Ma (Paces and Miller, 1993). The SLI was first described in detail by Stevenson (1974), who recognized its well-differentiated character. Between 1988 and 1990 the SLI was mapped by MGS as part of the USGS-sponsored Cooperative Geologic Mapping Program (COGEOMAP). A 1:24,000 geologic map of the SLI was compiled by Miller and others (1993), and the geology and petrology of the SLI was summarized in Miller and Ripley (1996) and Miller and Chandler (1997).

Although the exposed strike-length of the SLI is only about 3 km, it has a distinctive aeromagnetic signature that curves to the southwest for at least 20 km beneath a cover of glacial sediment (Miller and others, 1993). The nearly constant width of the aeromagnetic anomalies suggests that the intrusive sheet retains a uniform thickness and dip angle over most of the 20 km. At its eastern margin the SLI is truncated by a dike of Beaver River diabase, which has an emplacement age of 1095.8±1.2 Ma (Paces and Miller, 1993). The Beaver River diabase forms an extensive network of diabase sills and dikes, and is the most areally extensive unit within the Beaver Bay Complex. The SLI is also cut by a set of narrow dikes of incompletely mixed mafic to felsic rock (BRD-SLI hybrid dikes of Fig. 2A). These dikes probably represent hybrid mixtures of Beaver River diabase magma and residual felic melt from the SLI. At its base, on its northern margin, the SLI is in intrusive contact with a complex mixture of gabbroic to dioritic rocks,

---

Figure 2. **(A)** Geology of the Sonju Lake intrusion in the vicinity of Sonju Lake (after Miller and others, 1993), showing distribution of layered series rock units and location of drill core SNA-1 and outcrop samples from the preexisting MGS collection (see Tables 1 and 2). MR1 and MR2 indicate horizons that may reflect magmatic recharge events. SS is the horizon marking initial sulfide saturation. The line marked maaa is the internal datum plane, measured in meters above cumulus augite arrival (see text for discussion). The location of Figure 2B is shown by the boxed area. **(B)** Outcrop map for PGE-mineralized interval. Grey denotes areas of outcrop. North-south dashed lines show the two sampling traverses that cross the favorable interval. East-west dashed line marks the approximate trace of the horizon of initial sulfide saturation (see Fig. 4). The dashed gray line is the road. Location of outcrop samples is shown by black dots. Samples newly collected for this study have prefix SLP; other samples were obtained from preexisting MGS collections, and have various prefixes (Tables 1 and 2; see also Appendix Table 1). The map base is traced from U.S. Geological Survey Finland quadrangle, 7.5-minute series; the contour interval is 10 ft.

granophyric granite, and volcanic rocks (Fig. 2A). To the south, the top of the SLI is in gradational contact with quartz ferromonzodiorite of the Finland granite, which in turn grades up into leucogranite (Miller and others, 1993). The gradational contact between the SLI cumulates and the Finland granite probably reflects melting of the granite and mixing of the mafic and felsic magmas in the roof zone of the SLI.

The layered series of the SLI is composed of well-foliated mafic cumulates, which are sandwiched between a lower contact zone of melatroctolite (slmt) and an upper zone of olivine monzodiorite (slmd; Fig. 2A). Five units are distinguished within the layered series on the basis of successive cumulus arrivals of olivine (unit sld-dunite), plagioclase (unit slt-troctolite), augite (unit slg-gabbro), Fe-Ti oxides (unit slfg—Fe-Ti oxide gabbro), and apatite (unit slad- apatitic olivine diorite). It is also noteworthy that cumulus olivine is commonly absent from the Fe-Ti oxide gabbro unit (slfg). The cumulus appearance of a mineral is typically marked by its change from poikilitic to granular. The appearance of apatite is marked by a jump in its modal abundance from <0.5% to >3%. As profiled in drill core SLI-1 (Meints and others, 1993), the uppermost, well-foliated apatitic olivine diorite cumulates (unit slad) grade up into more massive, granophyric olivine monzodiorite, which forms the upper unit of the SLI (Fig. 3). The order in which cumulus phases appear is complemented by a smooth cryptic variation in the composition of olivine and augite (Fig. 3). These data indicate that the SLI formed by unidirectional fractional crystallization under nearly closed-system conditions. In other words, the SLI formed by continuous cumulus mineral accumulation at the floor of the magma chamber, and did not experience significant episodes of recharge, eruption, or assimilation.

Only two horizons in the SLI might indicate minor episodes of magma recharge (MR1 and MR2 in Figs. 2A and 3). MR1 is in the troctolite unit (slt), and is marked by the abrupt upsection decrease in grain size, amount of interstitial augite, and Fe/Fe+Mg of olivine. MR2 is in the Fe-Ti oxide gabbro unit (slfg), and is marked by pronounced modal layering and the reappearance of abundant olivine. Preliminary isotopic data (Vervoort, unpublished data) suggest limited contamination of the SLI by the Finland granite, but a more detailed study is in progress to determine the extent to which felsic roof rocks were assimilated by the SLI magma.

METHODS OF INVESTIGATION

In this study 67 samples from both outcrop and drill core were analyzed to create a representative geochemical profile of the 1.2-km-thick, south- and east-dipping SLI (Fig. 2A). Fifty of these samples were part of an existing MGS collection, and 17 were newly collected. Drill core was obtained from two drill holes that intersect the upper and lower contacts of the SLI (SNA-1 and SLI-1). Drill core SNA-1 is from an exploration drill hole that intersects the lowermost 180 m of the SLI. It is stored in the DNR core library in Hibbing, Minnesota. Drill core SLI-1 is approximately 230-m-long, and profiles the olivine monzodiorite (slmd) and apatitic olivine diorite (slad) units in the upper part of the SLI. Drill hole SLI-1 is located about 5 km west of the area of bedrock exposure shown in Figure 2B. It was drilled as part of a project to delineate the geology of the central Duluth Complex (Meints and others, 1993).

A total of 50 samples that represent the full thickness of the SLI were initially analyzed. These outcrop and drill-core samples were taken from the existing MGS collection obtained during previous field-based studies (Miller and others, 1993; see also Table 1, Table 2, and Appendix). Pt, Pd, and Au were analyzed by fire assay with an ICP-MS finish (detection limits of 0.1, 0.1, and 1 ppb respectively), and S was analyzed by XRF (detection limit 50 ppm, see Appendix). A combination of ICP and INAA major and trace element analyses, including Cu and Ni, were completed for

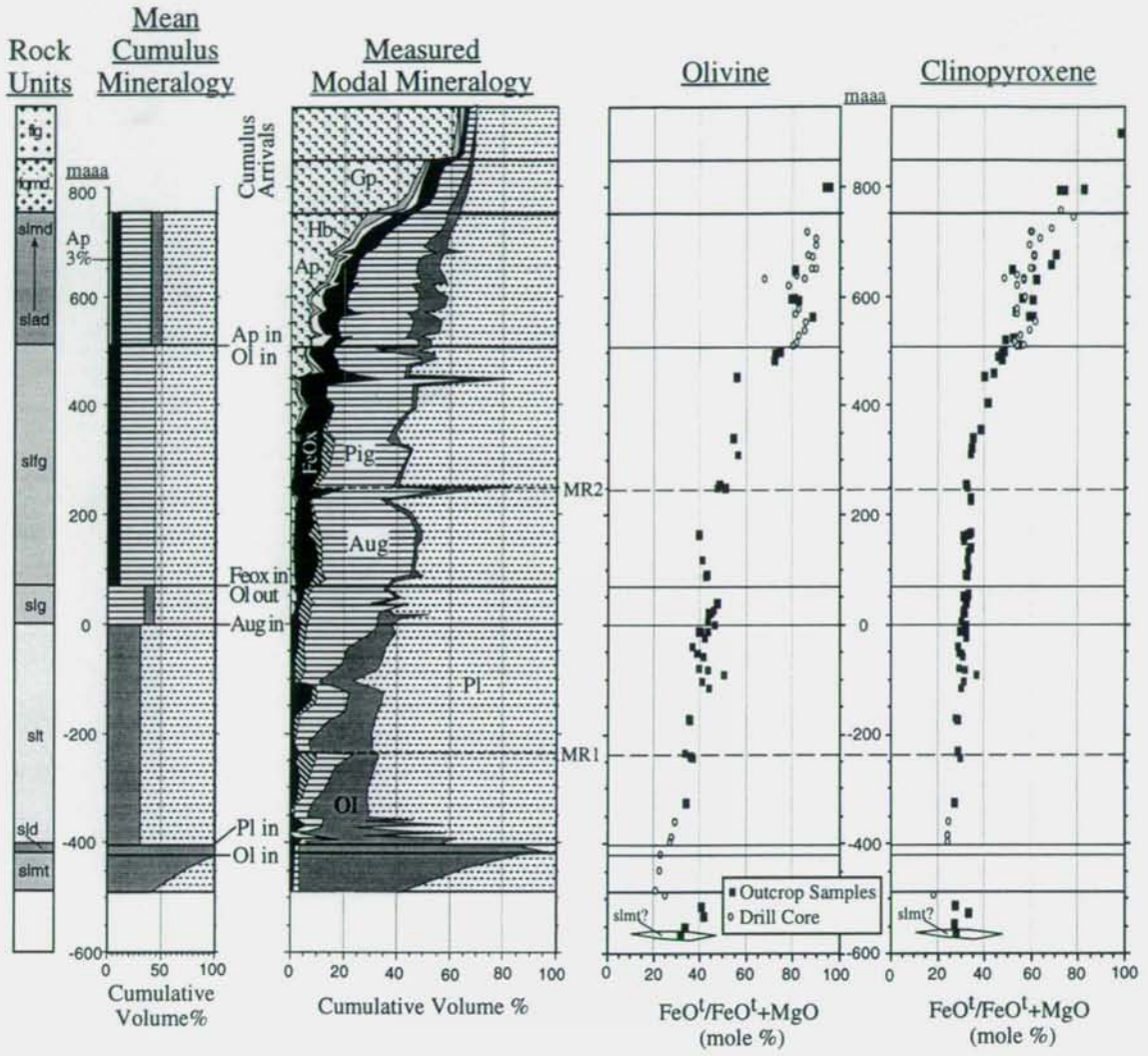

Figure 3. Stratigraphic variation in mean cumulus mineralogy, measured modal mineralogy, FeOt/FeOt+MgO ratio in olivine and augite in the SLI (after Miller and Ripley, 1996). Sample heights measured in meters above cumulus augite arrival (maaa). Outcrop sample data shown by black squares, drill-core data shown by open circles.

the initial 50 samples (see Appendix). When the results of the original 50 analyses were compiled, they clearly delineated a favorable PGE-enriched interval. A second set of 17 samples was then collected from two traverses across the favorable zone. Analyses of these 17 samples (SLP-1 through SLP-17; see Fig. 2B and Table 1) included INAA and ICP-MS analyses of 48 major and trace elements (including Cu and Ni); analysis of Pt, Pd, and Au by fire assay (with ICP-MS finish), and XRF analysis of S (see Appendix).

The analytical data obtained during this study were integrated with existing data from other sources (Table 1 and Appendix Table 1). The data were arranged in approximate stratigraphic order by projecting sample locations along strike to a common profile line. Although the orientation

Table 1. Summary of Geochemical Data for the Sonju Lake Intrusion

[data are arranged in inferred stratigraphic order, from base to top of intrusion; MR-1 and MR-2 are horizons that may record minor magma recharge events; analyses of outcrop samples from the traverse across the favorable interval are shown in bold; the shaded area represents the PGE-mineralized horizon; ppm, parts per million; ppb, parts per billion; .., no data; see Appendix for detection limits and complete geochemical analyses obtained in this study]

Sample number[1]	Strat. level in maaa[2]	rock unit[3]	Data Source[4]	S [ppm][5]	Cu [ppm][5]	Ni [ppm][5]	Pd [ppb][5]	Pt [ppb][5]	Au [ppb][5]	Cu/Pd	Pt+Pd [ppm]
SNA-553.5	-484	slmt	TS/UCLA	550	12	1018	..	..	..	..	..
SNA-531	-477	slmt	CG-XR	..	12	829	..	..	..	..	..
SNA-492	-464	slmt	TS/EL-BM	100	12	784	0.2	<0.1	5	6.00×10^4	<0.3
SNA-361	-424	slmt	EL-BM	..	10	798	..	..	..	..	..
SNA-340	-417	sld	TS	145	5	953	<0.1	<0.1	5	5.00×10^4	<0.2
SNA-338	-416	sld	EL-BM	..	1	763	..	..	..	..	..
SNA-312	-408	sld	EL-BM	..	4	1110	..	..	..	..	..
SNA-310	-408	sld	TS	405	57	1278	0.7	<0.1	3	8.14×10^4	<0.8
SNA-279	-398	slt	EL-BM	..	28	1220	..	..	..	..	..
SNA-276	-397	slt	TS	194	29	1228	2.1	<0.1	<1	1.38×10^4	<2.2
SNA-263	-393	slt	EL-BM	..	57	729	..	..	..	..	..
SNWR-4	-390	slt	EL-BM	..	40	421	..	..	..	..	..
SNWR-5	-382	slt	EL-BM	..	32	347	..	..	..	..	..
SNA-198	-373	slt	TS	287	26	709	0.7	<0.1	<1	3.71×10^4	<0.8
SNA-164	-362	slt	EL-BM	..	52	433	..	..	..	..	..
SNWR-20	-356	slt	EL-BM	..	40	444	..	..	..	..	..
SL15	-348	slt	MR-IS	..	45	760	..	..	..	..	..
SNA-102	-343	slt	TS	289	85	459	0.8	<0.1	<1	1.06×10^5	<0.9
SNA-33	-321	slt	EL-BM	..	69	189	..	..	..	..	..
SNWR-19	-317	slt	EL-BM	..	49	237	..	..	..	..	..
SNWR-21	-317	slt	EL-BM	..	40	419	..	..	..	..	..
SNWR-10	-310	slt	EL-BM	..	44	338	..	..	..	..	..
WSL6	-280	slt	TS	267	64	296	1.2	<0.1	<1	5.33×10^4	<1.3
SNWR-23	-254	slt	EL-BM	..	71	304	..	..	..	..	..
SNWR-8	-245	slt	EL-BM	..	83	264	..	..	..	..	..
D301A	-245	slt	TS	267	101	296	3.1	<0.1	123	3.26×10^4	<3.2
SL14	-242	slt	MR-IS	..	41	194	..	..	..	..	..
F222	-242	slt	CG-XR	..	11	202	..	..	..	..	..
MR-1(-240 maaa)											
SNWR-9	-238	slt	EL-BM	..	90	263	..	..	..	..	..
D301B	-234	slt	TS	..	29	360	1.1	<0.1	2	2.64×10^4	<1.2
SNWR-6	-183	slt	EL-BM	..	48	226	..	..	..	..	..
SL18	-173	slt	MR-IS	..	44	214	..	..	..	..	..
SNWR-7	-171	slt	EL-BM	..	37	187	..	..	..	..	..
WSL9	-168	slt	TS	202	29	252	0.8	<0.1	<1	3.63×10^4	<0.9
D290A	-132	slt	CG-XR	..	89	187	..	..	..	..	..
D281C	-116	slt	CG-XR	..	77	89	..	..	..	..	..
SNWR-12	-104	slt	EL-BM	..	94	168	..	..	..	..	..
D287	-104	slt	TS/UCLA	<50	47	160	3.9	0.4	2	1.21×10^4	4.3
D281	-83	slt	TS	..	97	204	0.4	<0.1	30	2.43×10^5	<0.5
SNWR-11	-66	slt	EL-BM	..	22	697	..	..	..	..	..
D288	-66	slt	TS	..	62	216	1.9	<0.1	2	3.26×10^4	<2
D291	-53	slt	CG-XR	..	61	274	..	..	..	..	..
WSL11	-53	slt	TS	269	68	204	2.0	<0.1	2	3.40×10^4	<2.1
F299D	-18	slt	CG-XR	..	..	183	..	..	..	..	..
WSL12	0	slt	TS	129	67	180	2.1	<0.1	<1	3.19×10^4	<2.2

Table 1. ctd...

Sample number[1]	Strat. level in maaa[2]	rock unit[3]	Data Source[4]	S [ppm][5]	Cu [ppm][5]	Ni [ppm][5]	Pd [ppb][5]	Pt [ppb][5]	Au [ppb][5]	Cu/Pd	Pt+Pd [ppm][5]
WSL10	5	slg	TS	96	75	123	1.8	<0.1	3	4.17×10^4	<1.9
F299B	6	slg	CG-XR	..	63	119	..	..	..	..	..
F295	21	slg	TS/CG-XR	..	65	178	1.9	<0.1	6	3.42×10^4	<2.0
SNRW-13	21	slg	EL-BM	..	54	82	..	..	..	..	..
SL13	29	slg	MR-IS	..	85	64	..	..	..	..	..
SNWR-14	38	slg	EL-BM	..	70	80	..	..	..	..	..
F300A	40	slg	TS	115	61	48	2.0	<0.1	<1	3.05×10^4	<2.1
F299A	50	slg	CG-XR	..	54	86	..	..	..	..	..
SL12	50	slg	MR-IS	..	87	54	..	..	..	..	..
HS14A	85	slfg	TS	..	60	90	3.5	<0.1	2	1.71×10^4	<3.6
F301D	88	slfg	CG-XR	..	44	151	..	..	..	..	..
SL11	90	slfg	MR-IS	..	57	83	..	..	..	..	..
WSL14	92	slfg	TS	76	54	84	1.0	<0.1	<1	5.40×10^4	<1.1
F335	168	slfg	TS	..	46	64	1.1	<0.1	<1	4.18×10^4	<1.2
SNWR-15	169	slfg	EL-BM	..	53	80	..	..	..	..	..
SL10	175	slfg	MR-IS	..	71	36	..	..	..	..	..
SLP-17	**187**	**slfg**	**TS**	**61**	**51**	**41**	**1.0**	**1.3**	**<1**	**5.10×10^4**	**2.3**
SNWR-16	224	slfg	EL-BM	..	67	29	..	..	..	..	..
F326	230	slfg	CG-XR	..	64	26	..	..	..	..	..
SLP-16	**231**	**slfg**	**TS**	**103**	**52**	**23**	**18.7**	**29.7**	**<1**	**2.78×10^3**	**48.4**
WSL19	233	slfg	TS	199	60	25	17.0	25.0	6	3.53×10^3	42.0
WSL20	235	slfg	TS	192	97	49	4.6	6.8	<1	2.11×10^4	11.4
F344	240	slfg	CG-XR	..	88	26	..	..	..	..	..
SLP-11	**247**	**slfg**	**TS**	**149**	**89**	**16**	**5.7**	**3.1**	**<1**	**1.56×10^4**	**8.8**
F328	252	slfg	TS	..	79	16	16.0	23.0	3	4.94×10^3	39.0
				MR-2 (255 maaa)							
SL9	256	slfg	MR-IS	..	60	94	..	..	..	..	..
F231	256	slfg	TS	<50	57	112	5.1	12.0	5	1.12×10^4	17.1
SLP-15	**259**	**slfg**	**TS**	**108**	**37**	**22**	**6.5**	**5.5**	**<1**	**5.69×10^3**	**12.0**
SLP-10	**260**	**slfg**	**TS**	**79**	**80**	**59**	**7.0**	**1.8**	**2**	**1.14×10^4**	**8.8**
SLP-9	**278**	**slfg**	**TS**	**135**	**102**	**26**	**21.4**	**2.5**	**<1**	**4.77×10^3**	**23.9**
F332	280	slfg	TS	..	71	63	6.8	5.6	<1	1.04×10^4	12.4
SLP-8	**290**	**slfg**	**TS**	**127**	**78**	**34**	**19.1**	**4.8**	**<1**	**4.08×10^3**	**23.9**
F334A	295	slfg	TS	..	85	32	36.0	2.8	3	2.36×10^3	38.8
SLP-7	**296**	**slfg**	**TS**	**160**	**78**	**22**	**293.0**	**0.9**	**<1**	**2.66×10^2**	**293.9**
SLP-14	**304**	**slfg**	**TS**	**89**	**30**	**6**	**133.0**	**4.6**	**<1**	**2.26×10^2**	**137.6**
SLP-6	**316**	**slfg**	**TS**	**63**	**82**	**13**	**179.0**	**0.4**	**<1**	**4.58×10^2**	**179.4**
F411	321	slfg	TS/UCLA	<50	72	15	320.0	66.0	6	2.25×10^2	386.0
				level of initial sulfide saturation							
SLP-5	**323**	**slfg**	**TS**	**70**	**514**	**14**	**<0.1**	**6.0**	**12**	**5.14×10^6**	**<6.1**
SLP-4	**339**	**slfg**	**TS**	**59**	**618**	**9**	**0.5**	**2.1**	**4**	**1.24×10^6**	**2.6**
F330	341	slfg	TS	..	630	9	0.3	<0.1	27	2.10×10^6	<0.4
SL8	355	slfg	MR-IS	..	513	8	..	..	..	..	..
SLP-3	**356**	**slfg**	**TS**	**68**	**402**	**5**	**1.0**	**2.1**	**85**	**4.02×10^5**	**3.1**
WSL15	357	slfg	TS	375	406	2	0.5	<0.1	2	8.12×10^5	<0.6
SLP-12	**370**	**slfg**	**TS**	**216**	**375**	**5**	**1.4**	**1.3**	**<1**	**2.68×10^5**	**2.7**
SLP-1	**371**	**slfg**	**TS**	**505**	**515**	**5**	**0.8**	**1.8**	**5**	**6.44×10^5**	**2.6**
SLP-2	**377**	**slfg**	**TS**	**170**	**473**	**4**	**0.9**	**2.1**	**<1**	**5.26×10^5**	**3**
SLP-13	**398**	**slfg**	**TS**	**90**	**368**	**6**	**0.9**	**2.0**	**2**	**4.09×10^5**	**2.9**
F395	404	slfg	CG-XR	..	540	15	..	..	..	..	..
F395R	?	slfg	TS	..	96	10	17.0	22.0	2	5.65×10^3	39.0
F397	420	slfg	CG-XR	..	526	14	..	..	..	..	..
F407	452	slfg	TS	..	1865	12	<0.1	<0.1	3	1.87×10^7	<0.2

Table 1. ctd...

Sample number[1]	Strat. level in maaa[2]	rock unit[3]	Data Source[4]	S [ppm][5]	Cu [ppm][5]	Ni [ppm][5]	Pd [ppb][5]	Pt [ppb][5]	Au [ppb][5]	Cu/Pd	Pt+Pd [ppm][5]
F322L	459	slfg	TS	134	223	2	<0.1	<0.1	3	2.23 x 10^6	<0.2
SL7	483	slfg	MR-IS	..	522	14	..	..	..	..	..
F229	483	slfg	TS	540	432	2	<0.1	<0.1	<1	4.32 x 10^6	<0.2
F408	491	slfg	CG-XR	..	597	18	..	..	..	..	..
F322A	498	slfg	TS	..	371	2	<0.1	<0.1	<1	3.71 x 10^6	<0.2
SLI-874	510	slad	CG-XR	..	64	11	..	..	..	..	..
SLI-862	514	slad	CG-XR	..	55	12	..	..	..	..	..
F322C	524	slad	TS	403	367	2	<0.1	<0.1	20	3.67 x 10^6	<0.2
SLI-830	525	slad	TS/CG-XR	2550	77	18	0.2	<0.1	<1	3.85 x 10^5	<0.3
SLI-802	534	slad	CG-XR	1780	78	<1	..	..	..	..	..
SLI-787	539	slad	CG-XR	..	78	10	..	..	..	..	..
SLI-748	552	slad	CG-XR	..	64	9	..	..	..	..	..
F310	562	slad	MR-IS	..	561	12	..	..	..	..	..
SLI-693	570	slad	CG-XR	..	74	14	..	..	..	..	..
SLI-641	587	slad	CG-XR	..	53	14	..	..	..	..	..
F311	595	slmd	TS/UCLA	1595	168	2	<0.1	<0.1	2	1.68 x 10^6	<0.2
F390A	595	slmd	CG-XR	..	179	12	..	..	..	..	..
SL4	599	slmd	MR-IS	..	256	10	..	..	..	..	..
SL3	603	slmd	MR-IS	..	104	11	..	..	..	..	..
SLI-586	605	slmd	TS/CG-XR	1055	55	12	<0.1	<0.1	<1	5.55 x 10^5	<0.2
SLI-559	614	slmd	CG-XR	..	69	16	..	..	..	..	..
SLI-538	620	slmd	CG-XR	..	100	14	..	..	..	..	..
SLI-518	627	slmd	CG-XR	..	113	6	..	..	..	..	..
F312	631	slmd	TS/CG-XR	650	326	3	<0.1	<0.1	5	3.26 x 10^6	<0.2
SLI-505	631	slmd	CG-XR	..	104	18	..	..	..	..	..
SLI-499	633	slmd	CG-XR	..	113	27	..	..	..	..	..
SL2	637	slmd	MR-IS	..	50	10	..	..	..	..	..
SLI-457	647	slmd	TS/CG-XR	1910	63	6	<0.1	<0.1	3	6.35 x 10^5	<0.2
F319	650	slmd	CG-XR	..	107	2	<0.1	<0.1	3	1.07 x 10^6	<0.2
SL1	656	slmd	MR-IS	..	44	11	..	..	..	..	..
SLI-382	672	slmd	CG-XR	..	76	9	..	..	..	.	..
F325	674	slmd	TS/CG-XR	105	43	5	<0.1	<0.1	4	4.30 x 10^5	<0.2
SLI-318	693	slmd	TS/CG-XR	2860	81	5	<0.1	<0.1	3	8.15 x 10^5	<0.2
SLI-242	718	slmd	TS/CG-XR	3150	69	5	1.1	<0.1	3	6.32 x 10^4	1.2
SLI-222	724	slmd	CG-XR	..	43	<1	..	..	..	..	..
SLI-200	731	slmd	CG-XR	..	57	<1	..	..	..	..	..
SLI-188	735	slmd	CG-XR	..	56	<1	..	..	..	..	..
SLI-120	758	fqmd	CG-XR	..	43	<1	..	..	..	..	..
E250	800	fqmd	TS/CG-XR	241	17	2	<0.1	<0.1	3	1.70E x 10^5	<0.2
E246	850	fqmd	TS/UCLA	780	23	2	..	..	..	..	..
E234	900	flg	TS/CG-XR	360	19	2	..	..	..	..	..
F140	950	flg	TS/CG-XR	<50	14	2	0.2	0.6	<1	7.25 x 10^4	0.8

[1] location (UTM coordinates) of samples analyzed for this study is given in Tables 2 and 3

[2] maaa - meters above cumulus augite arrival (slt-slg contact)

[3] shows abbreviation for rock unit; see text for description

[4] geochemical data from following sources; multiple analyses are recorded for some samples

TS: this study; analysed by Activation Laboratories Ltd., Ancaster, Ontario, Canada; see Appendix

CG-XR: Unpublished data acquired for the COGEOMAP project; analysed by X-Ray Assay Labs (XRAL), Don Mills, Ontario

MR-IS: INAA analyses from Rogge (1989)

UCLA: Unpublished INAA analyses conducted at UCLA; analyst—Eric Jerde

EL-BM: Unpublished data from drill core and outcrop samples given to the MGS by E.K. Lehmann and Associates Inc. in 1988; used here with permission; drill core and data stored at DNR-Hibbing; analyses conducted in 1983 by Barringer-Magenta, Rexdale, Ontario, Canada

[5] for detection limits see Appendix

Table 2. Location of 50 outcrop and drill-core samples from preexisting MGS collection

[given in Universal Transverse Mercator (UTM) coordinates]

Sample Number	UTM Easting	UTM Northing
D281	635859	5260840
D287	635131	5260901
D288	635085	5260794
D301A	635277	5261330
D301B	635254	5261292
E234	633229	5256404
E246	632644	5257756
E250	633895	5258449
F140	630799	5252738
F229	634115	5259420
F231	633764	5260060
F295	634112	5260648
F300A	635471	5260489
F311	633866	5259270
F312	633674	5259192
F319	631807	5259458
F322A	633758	5259449
F322C	633759	5259405
F322L	633766	5259530
F325	634016	5258916
F328	633403	5260135
F330	633669	5259842
F332	632838	5260149
F334A	632554	5260092
F335	633836	5260265
F395	634189	5259545
F407	633966	5259522
F411	633923	5259878
HS14A	633770	5260500
SLI 242	627311	5257514
SLI 318	627311	5257514
SLI 457	627311	5257514
SLI 586	627311	5257514
SLI 830	627311	5257514
SNA 101.5	634912	5261559
SNA 198	634912	5261559
SNA 276	634912	5261559
SNA 310	634912	5261559
SNA 340	634912	5261559
SNA 492	634912	5261559
SNA 554	634912	5261559
WSL6	635311	5261451
WSL9	635312	5261116
WSL10	635418	5260614
WSL11	635450	5260731
WSL12	635435	5260638
WSL14	633756	5260475
WSL15	634074	5259728
WSL19	633842	5260112
WSL20	633863	5260128

Table 3. Location of 17 outcrop samples collected from the favorable zone

[given in Universal Transverse Mercator (UTM) coordinates]

Sample Number	UTM Easting	UTM Northing
SLP-1	633829	5259725
SLP-2	633836	5259729
SLP-3	633875	5259779
SLP-4	633845	5259830
SLP-5	633852	5259874
SLP-6	633844	5259894
SLP-7	633860	5259933
SLP-8	633863	5259948
SLP-9	633850	5259981
SLP-10	633857	5260020
SLP-11	633859	5260048
SLP-12	633456	5259855
SLP-13	633433	5259771
SLP-14	633449	5259961
SLP-15	633413	5260131
SLP-16	633434	5260205
SLP-17	633454	5260300

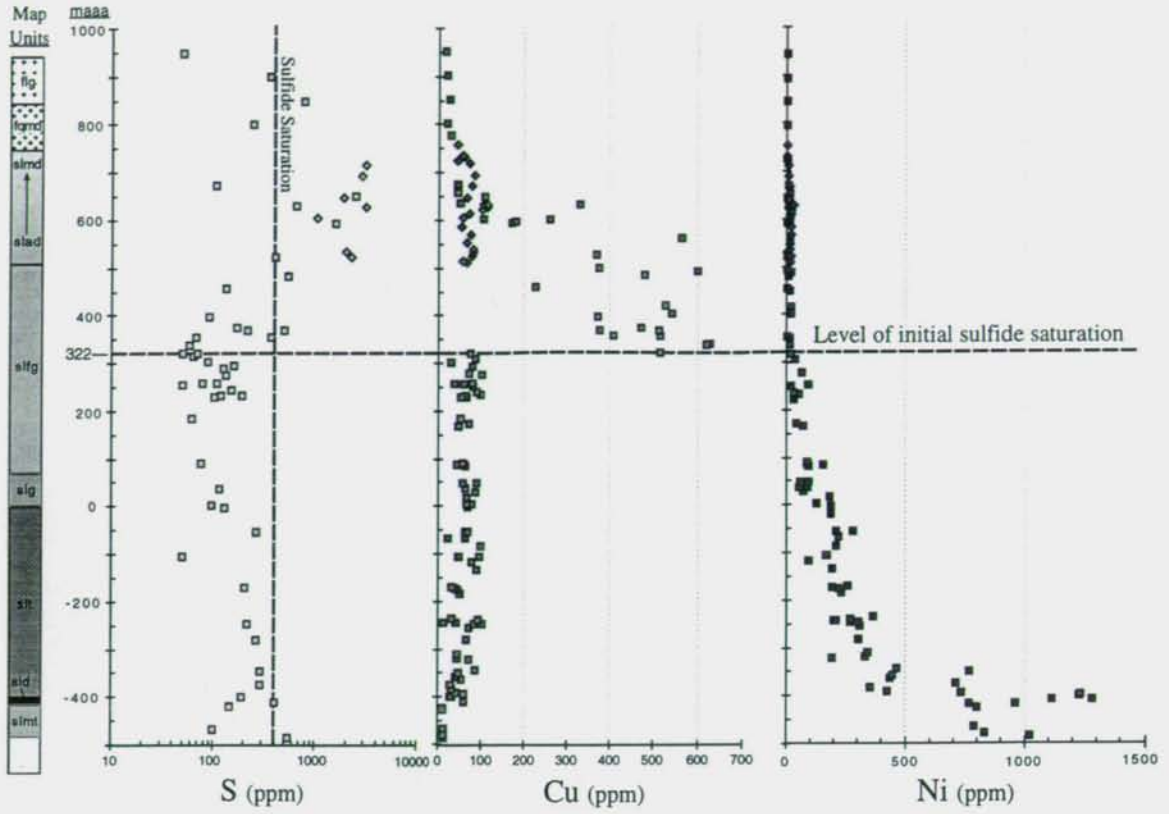

Figure 4. Stratigraphic variation in sulfur, copper, and nickel abundance in the SLI. Heavy dashed horizontal line denotes level of initial sulfide saturation based on abrupt increase in Cu abundance at 322 maaa. Heavy dashed vertical line in S plot denotes minimum concentration of S (400 ppm) considered from theoretical grounds (Boudreau and McCallum, 1992) to indicate sulfide saturation in gabbroic cumulates. Samples from drill core SLI-1 shown as diamonds; samples from outcrop and drill core SNA-1 shown as squares. Data listed in Table 1.

of layering or foliation (or both) was measured for most samples, there may be some inaccuracy in the projected stratigraphic position of each sample, due to local variations in internal structure, and minor faults with uncertain amounts of offset. The stratigraphic position of a sample within the intrusion is based on its height in meters above or below the sharp horizon where augite changes from intercumulus (poikilitic) to cumulus (granular), and is reported in maaa (meters above cumulus augite arrival). Correlation between SLI-1 drill-core and outcrop samples from the upper part of the SLI is not straightforward due to poor exposure, structural complications in the exposed part of the intrusion, and the lack of a definitive datum horizon in the drill core (Fig. 2A; see also Miller and others, 1993; Meints and others, 1993). The base of the drill core is estimated to be close to the horizon marking the cumulus arrival of apatite. In stratigraphic plots of the geochemical data (Figs. 4–6), the SLI-1 drill core samples are distinguished from outcrop and SNA-1 drill-core samples by different symbols.

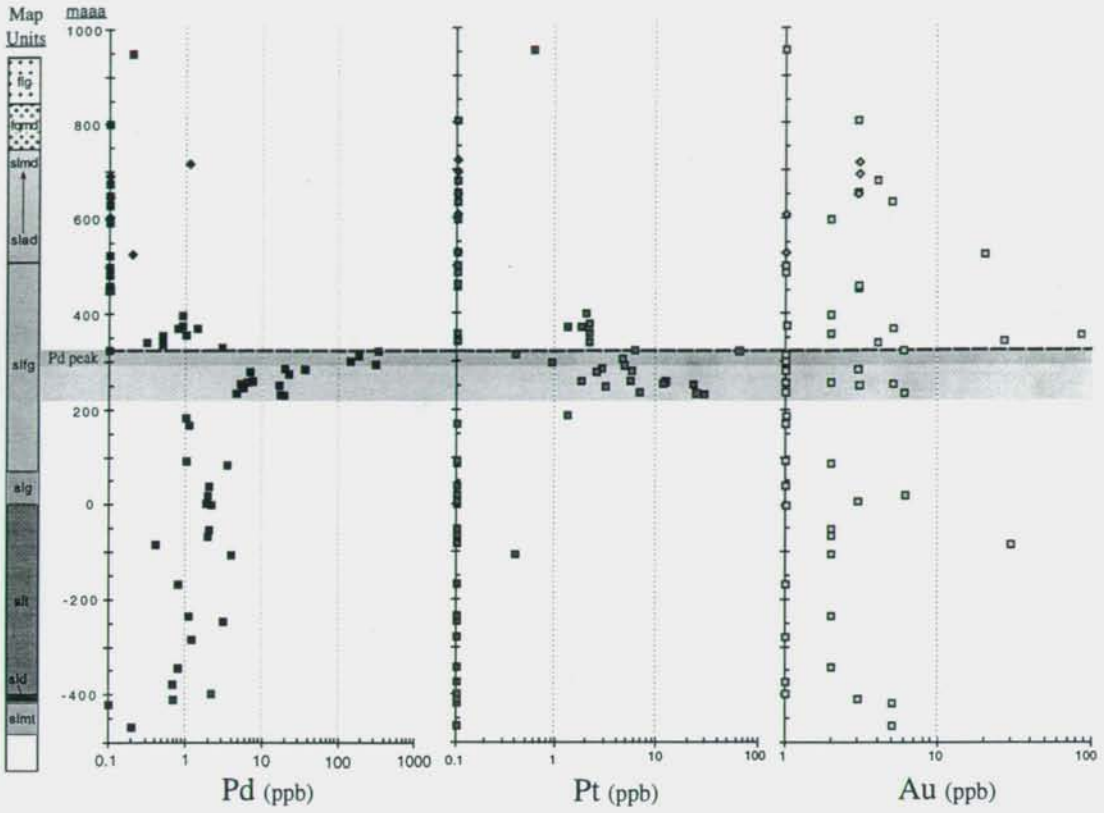

Figure 5. Stratigraphic variation in palladium, platinum, and gold abundance in the SLI. Heavy dashed horizontal line denotes level of initial sulfide saturation based on abrupt increase in Cu abundance at 322 maaa (Fig. 4). Dark shaded zone denotes 25-m-thick interval containing Pd >100 ppb. Lighter shaded zone denote samples with 5-100 ppb Pd. Samples from drill core SLI-1 shown as diamonds; samples from outcrop and drill core SNA-1 shown as squares. Data listed in Table 1.

RESULTS AND INTERPRETATION

The geochemical data clearly and convincingly show that conditions required for the development of a stratiform PGE horizon were fulfilled by the SLI magma system. The SLI magma was initially sulfide undersaturated, and it experienced a considerable degree of fractional crystallization. After sulfide saturation and segregation of sulfide melt, the remaining silicate magma was strongly depleted in PGEs.

Theoretical and experimental data on the solubility of sulfide in a silicate melt indicates that when a tholeiitic mafic magma is saturated in sulfide, it should crystallize a rock that contains at least 400 ppm S (Boudreau and McCallum, 1992). Use of the benchmark S concentration of 400 ppm to determine the level in the layered intrusion at which sulfide saturation of the magma first took place leads to ambiguous conclusions. The whole rock S data from the SLI (Fig. 4) generally indicate that the parent magma was initially sulfide undersaturated but became saturated during

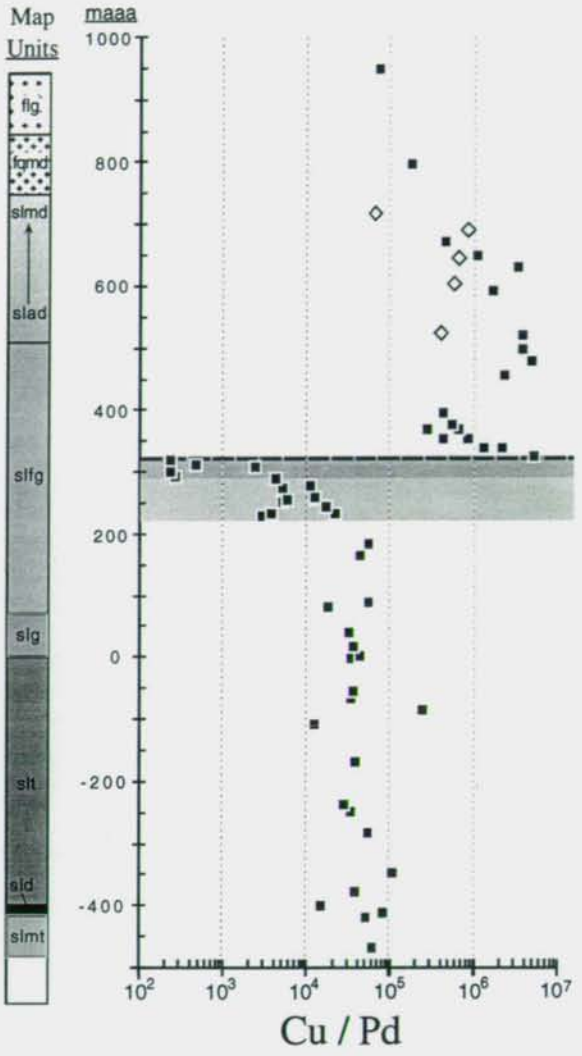

Figure 6. Stratigraphic variation in Cu/Pd ratio in the SLI. Heavy dashed horizontal line denotes level of initial sulfide saturation based on abrupt increase in Cu abundance at 322 maaa (Fig. 4). Dark and light shaded zones denote Pd-rich interval as shown in Figure 5. Samples from drill core SLI-1 shown as diamonds; samples from outcrop and drill core SNA-1 shown as squares. Data listed in Table 1.

crystallization of the Fe-Ti oxide gabbro unit (slfg). Between 350 and 480 maaa the S concentrations vary; they range between 68 ppm and 505 ppm (Figure 4 and Table 1). The S data could be interpreted to indicate that initial sulfide saturation of the magma was not sustained. However, such an intermittent state of sulfide saturation is not consistent with the largely closed nature of the SLI system, as indicated by other petrologic data. Indeed, the copper data suggest that the sulfur data do not accurately reflect the sulfide-saturated state of the magma.

Copper concentration increases abruptly from <100 ppm to >500 ppm at the 322 maaa level, which is 35 m below the level at which the S concentration first approaches 400 ppm. The sustained, although decreasing, Cu concentration upsection of the 322-maaa level is consistent with a closed system in which sulfide saturation (once achieved) persisted throughout crystallization. The gradual decrease in Cu concentration above the 322-maaa level would in this case reflect fractional exsolution of Cu-enriched sulfide melt from the sulfide-saturated magma. When compared with the outcrop samples for the upper SLI units, samples from the lower half of the SLI-1 drill core (Fig. 4) have consistently lower Cu concentrations. This disparity could indicate inaccurate correlation between

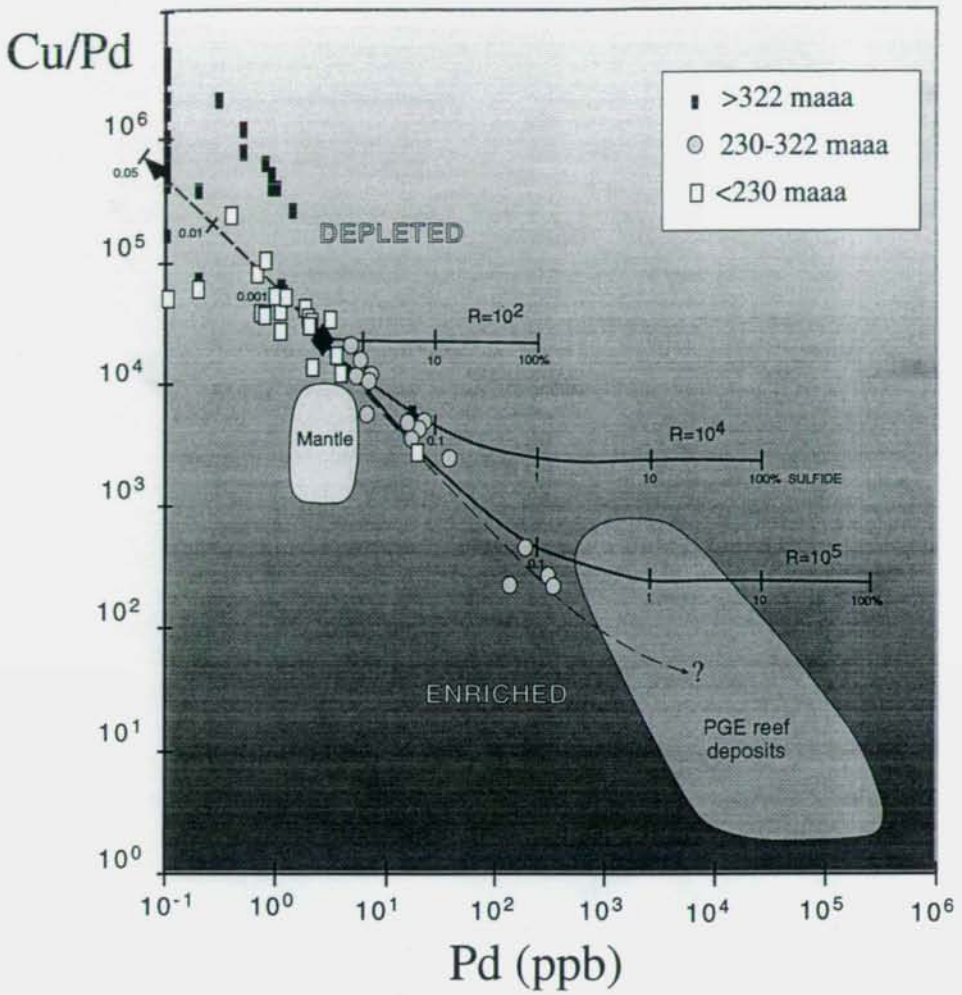

Figure 7. Plot of Cu/Pd ratio vs. Pd concentration for SLI samples. General stratigraphic positions of samples relative to 230 and 322 maaa are denoted by different symbols. Black diamond denotes possible SLI parental magma composition. Solid curves show composition paths for sulfide exsolved from parental compositions with R-factors (silicate/sulfide ratios) of 10^2, 10^4 and 10^5 (from Barnes and others, 1993); the curves are scaled for weight percent sulfide in rock sample. Heavy dashed curve denotes composition path of the magma as progressively more sulfide is exsolved (in wt. percent). Light dashed line is a projection of SLI data toward possible PGE reef compositions. The composition fields shown for undepleted mantle-derived magma and various PGE reef deposits are also shown (from Barnes and others, 1993).

samples. Alternatively, the observed geochemical differences may indicate some lateral variability in the efficiency of sulfide exsolution. If so, this may also have implications for the lateral variability in PGE concentration.

It is puzzling that S concentration does not show an abrupt increase similar to that shown by Cu at 322 maaa. The possibility that this may indicate inaccurate S analyses can be discounted by cursory petrographic observations of polished sections from this interval; petrographic observations confirm that samples with low S concentrations correspond to those low in sulfide minerals. The most likely explanation for the S concentrations documented for this interval is that samples with low S and high Cu concentrations reflect dissolution of sulfide by deuteric fluids

that did not mobilize Cu. Such a phenomenon can occur if the fluid/rock partition coefficients for Cu are much lower than for S, as appears to be true for Cl-rich fluids (Boudreau and McCallum, 1992). The Fe-Ti oxide gabbro (unit slfg) contains petrographic evidence for such fluids in the form of uralitized pyroxene and local concentrations of secondary chlorite and amphibole. A consequence of a selective dissolution process is that it should result in more Cu-rich sulfides in these Cu-rich/S-poor samples. Studies are underway to determine if such Cu-rich sulfides are present. Another consequence of this selective dissolution process, is that if such fluids were incapable of moblilizing Cu, they should also have been incapable of moving other metals as well.

Nickel (Ni) concentration decreases upsection in the SLI, and is markedly low at the inferred level of sulfide saturation (Fig. 4), and remains low (1-27 ppm) in overlying units. The Ni depletion can be attributed to extensive olivine crystallization during formation of the dunite (sld) and troctolite (slt) units. The overall decrease in Ni concentration, and the lack of any major increase in its concentration are consistent with the SLI magma being closed to any significant inputs of new magma during its crystallization.

Palladium (Pd), platinum (Pt), and gold (Au) consistently peak in abundance between 220 and 360 maaa, near the level of initial sulfide saturation. The stratigraphic variation in Pd concentration is particularly interesting. The peak Pd concentrations of 100–320 ppb lie within a 25-m-thick interval (Fig. 5) just below the 322 maaa sulfide saturation level (as interpreted from the Cu data, Fig. 4). Palladium concentrations below the peak Pd interval generally run between 0.5–3 ppb, although in the 50 m below the peak Pd interval, the concentration of Pd increases upsection from 1–2 ppb to as much as 36 ppb. Palladium concentrations below 3 ppb probably reflect minor amounts (10–30 percent) of PGE-undepleted intercumulus magma that became trapped within the framework of cumulus minerals on the magma chamber floor. The gradual increase in concentration of Pd below the peak interval may reflect the enrichment of PGEs in the magma due to fractional crystallization, and the approach of the magma to sulfur saturation. Above the peak Pd interval, Pd concentration decreases to below the limit of detection (<0.01 ppb). Platinum concentrations only rise above the limit of detection (i.e. > 0.1 ppb) in the 200 meters straddling the Pd peak interval. The highest Pt concentration (66 ppb) is recorded in the sample that has the highest Pd concentration (320 ppb). Platinum concentration also shows a secondary peak 90 m below the main Pd and Pt peaks. The Au concentration varies less systematically than Pd and Pt, although the highest Au concentration (85 ppb) is 35 m above the peak Pd-Pt interval. The position of peak PGE concentration just below peak Cu concentration (Figs. 4 and 5) indicates that PGEs were scavenged from the SLI magma by the first batch of sulfide melt that settled to the 320 maaa level of crystallization.

The efficiency with which PGEs were scavenged from the SLI magma by sulfides is indicated by (1) the very low concentration (typically below the limit of detection) of Pd and Pt above their peak interval (Fig. 4), and (2) the nearly four orders-of-magnitude increase in the Cu/Pd ratio across the sulfide-saturation horizon (Fig. 6). The increase in the Cu/Pd ratio reflects that fact that Pd is several orders of magnitude more compatible with sulfide melt than with silicate melt, when compared to Cu (Barnes and others, 1993). Thus, the more efficient the sulfide melt is at scavenging PGEs from the silicate magma, the greater the increase in the Cu/Pd ratio. The sudden and large increase in the Cu/Pd ratio strongly suggests that PGEs were efficiently concentrated in the narrow horizon that marks the first arrival of sulfide melt at the magma chamber floor. It is probable that the samples collected thus far do not include this horizon, which most likely lies in the 7-m-thick interval between samples SLP-5 and SLP-6 (eastern traverse line, Fig. 2B; 316–323 maaa; Table 1).

Another way to evaluate the efficiency with which PGEs are scavenged is to compare Cu/Pd ratios and Pd concentrations (Fig. 7, and Barnes and others, 1993). A comparison of these two

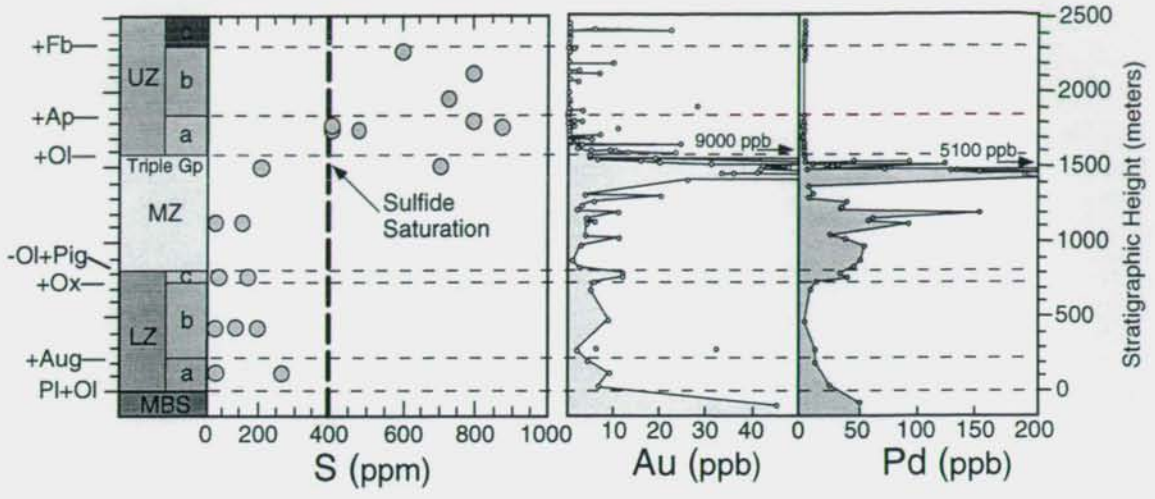

Figure 8. Stratigraphic variation of sulfur, gold and palladium in the Skaergaard intrusion (after Andersen and others, 1998). Major stratigraphic map units based on cumulus mineral arrivals are shown in left hand column. Heavy dashed line at S = 400 ppm marks the minumum concentration of sulfur theoretically calculated to indicate sulfide saturation in gabbroic cumulates (Boudreau and McCallum, 1992)

data sets shows the effect that different silicate/sulfide melt ratios (R-factors) and sulfide concentrations (wt. percent) have on the Cu/Pd ratio and Pd concentration in the intrusive rocks that crystallized (Fig. 7). The data for the lower part of the SLI plot in the area of the graph that represents slightly depleted Cu/Pd ratios relative to mantle values. This implies that the SLI parent magma may have experienced some PGE depletion prior to its emplacement into the Beaver Bay Complex. A high PGE concentration could have been reestablished during the fractional crystallization that preceeded the initial sulfide-saturation event. Samples from as far as 90 m below the sulfide-saturation horizon lie on a curve that corresponds to a silicate/sulfide melt ratio of $>10^5$. This large R-factor (high silicate/sulfide melt ratio) implies that each bleb of sulfide melt scavenged PGEs from a relatively a large volume of silicate melt as the sulfide melt descended to the magma chamber floor. The decrease in the Cu/Pd ratio, and the increase in Pd concentration as the sulfide-saturation horizon is approached (Figs. 5 and 6) indicate that the peak Pd grade associated with the initial sulfide-saturation horizon may be comparable to other economic PGE-reef deposits (projected arrow in Fig. 7). Again, it is unlikely that the PGE-enriched sulfide-saturation horizon was sampled in this study.

COMPARISON TO THE SKAERGAARD INTRUSION

The geochemical and petrologic similarities between the SLI and the Skaergaard Intrusion of East Greenland are remarkable, and bode well for the SLI hosting a PGE reef of a grade comparable to the Platinova reef (Fig. 8). Both intrusions have similar closed-system crystallization histories, and similar cumulus mineral sequences. Both intrusions formed from parent magmas that were initially sulfide-undersaturated, but became saturated at proportionally similar stratigraphic levels (when they were approximately 60 percent crystallized; compare Figures 4 and 8, and note that the Skaergaard is nearly twice the thickness of the SLI). Moreover, both intrusions were crystallizing a cumulus mineral assemblage that included plagioclase + augite + iron oxide at the time of sulfide saturation. Similarities in the changes in Pd concentration with stratigraphic position are also

particularly striking (Figs. 5 and 8). Both intrusions show low and variable concentrations of Pd in their lower, sulfide-undersaturated portion, which probably reflects variable amounts of trapped undepleted magma. Both intrusions also show almost complete Pd depletion above the sulfide-saturation horizon. In the SLI peak Au concentration appears to be displaced upward from Pd peak concentration. A similar displacement of Pd and Au peak concentrations is documented for the Platinova reef (Fig. 8), and is especially pronounced in the interior of the bowl-shaped Skaergaard intrusion (Andersen and others, 1998).

The SLI and Skaergaard intrusions differ in that the SLI crystallized from the floor upward, whereas the Skaergaard crystallized both downward from its roof zone to create an upper border series, as well as upward from the floor. Because the SLI underplated and partially melted the overlying granitic body, there was no substrate against which an upper border series could attach (e.g. Marsh, 1988). It is not clear whether the presence of a felsic melt above the SLI magma affected sulfide saturation and PGE mineralization. Stable and radiogenic isotope analyses are underway to address this question.

A more significant difference between the intrusions may be that of scale. The Platinova reef of the Skaergaard consists of as many as 10 mineralized intervals (each of which is as much as several meters thick) that are spread over a stratigraphic thickness of 60 meters (Andersen and others, 1998). The highest PGE concentrations (5100 ppb Pd and 400 ppb Pt) are recorded in the lowest interval, and each successive interval is less PGE enriched. The mineralized intervals lie within the Triple Group, which is an interval of macrocyclic, modally layered lecocratic and melanocratic gabbro. Andersen and others (1998) conclude that the macrocyclic modal layering and the PGE mineralization are not genetically linked. At the scale at which the geochemically favorable horizon in the SLI has been mapped and sampled, it does not display either a lithologic cyclicity or a mineralization pattern comparable to that documented in the Skaergaard, although drilling and detailed geochemical analyses are necessary to confirm this.

CONCLUSIONS AND RECOMMENDATIONS

The results of this geochemical study strongly indicate that significant stratiform PGE mineralization exists in the medial part of the SLI. If the PGE reef in the SLI is comparable in scale to other reefs, it is likely to be a meter or two thick (Naldrett, 1993). Because samples from the traverse across the favorable horizon are separated from each other by 2–8 m, core drilling and systematic geochemical sampling will be necessary to establish the exact position, peak grade, thickness, and lateral continuity of the reef. It is recommended that exploration drilling be targeted at the 320 maaa level in the exposed eastern part of the intrusion, and at comparable levels in the unexposed SLI to the west (Miller and others, 1993). The location of the PGE reef may not be macroscopically obvious (total sulfide minerals may be less than 1 modal percent), so widely spaced samples should be analyzed for Cu and S in order to locate the initial sulfide-saturation horizon, and thus the level of peak PGE mineralization.

Beyond specific details regarding mineralization within the SLI, this study—together with that conducted on the Layered Series at Duluth (Miller, 1998a,b)—has favorable implications for the existence of stratiform PGE mineralization in tholeiitic layered intrusions in northeastern Minnesota.

1. These studies demonstrate that a general set of geochemical criteria can be used to evaluate the overall potential for stratiform PGE mineralization in tholeiitic layered intrusions, and to identify favorable intervals for PGE mineralization within individual

intrusions. It may be sufficient to determine the stratigraphic variability in Cu and S concentrations (as indicators of sulfide saturation during the crystallization history of an intrusion) in order to locate a favorable horizon for a PGE reef.

2. These studies suggest that all well-differentiated tholeiitic layered intrusions that became sulfide saturated in the latter stages of their crystallization have the potential to host stratiform PGE reefs, regardless of whether they evolved as an open (DLS) or closed (SLI) magmatic system. The Duluth and the Beaver Bay complexes contain a number of well-differentiated tholeiitic layered intrusions that provide inviting exploration targets. Given that intrusions such as the DLS and the SLI were both initially sulfide undersaturated, it can be reasonably presumed that most intrusions of the Duluth and Beaver Bay complexes were similarly undersaturated at the time of their emplacement.

The well-differentiated tholeiitic layered intrusions that occur in areas open to exploration in northeastern Minnesota are noted in Figure 1. In addition to the SLI and the DLS, these intrusions include (1) the large Greenwood Lake intrusion of the Duluth Complex, (2) the small, plug-like Osier Lake intrusion of the Duluth Complex, (3) the Pequayan Lake intrusion of the Duluth Complex, (4) the differentiated cycles of the Cloquet Lake layered series of the Beaver Bay Complex, and (5) the northeastern, differentiated part of the Houghtaling Creek troctolite of the Beaver Bay Complex. With the exception of the Houghtaling Creek troctolite, which is relatively well exposed (Boerboom and Miller, 1994; Miller and others, 1994), all the other intrusions are poorly exposed or unexposed. They are known mainly from their aeromagnetic signature and widely scattered drill holes. A recently published 1:100,000 geologic map of the central Duluth Complex and western Beaver Bay Complex (Miller and Chandler, 1999) delineates and describes these intrusions, and shows outcrop and drill hole locations. Although there may be some hesitance regarding exploration in these unexposed intrusions, the stratiform nature of a potential PGE reef means that only one geochemical profile is required to evaluate the sulfide-saturation character of an intrusion, and thereby identify a favorable horizon for detailed sampling. Geophysical surveys (such as electromagnetic or induced polarization surveys) across these intrusions could be used to assess where sulfide concentration increases markedly. The attractiveness of this type of stratiform mineralization is that once a favorable horizon is identified, further exploration simply becomes a matter of following the reef along strike and down dip.

Ironically, the two intrusions where most PGE exploration activity has been focused until now (the Partridge River and South Kawishiwi intrusions, Fig. 1), may hold the least potential for the type of PGE mineralization described here, because they are not well differentiated, and were contaminated by extramagmatic sulfur during emplacement. These very open-system intrusions did not differentiate beyond crystallization of olivine-plagioclase cumulates (Severson, 1998; Miller and Ripley, 1996). Although the stratiform PGE mineralization found at the Birch Lake prospect in the South Kawishiwi intrusion may seem to contradict this conclusion, the style of mineralization is not of the type described here. The Birch Lake PGE-Cr mineralized horizon is indicative of processes that include magma recharge, iron-formation assimilation, and late stage remobilization of PGEs and Cr by Cl-brines along fault zones (Hauck, Severson, Zanko and others, 1997; Hauck, Severson, Ripley and others, 1997).

The discovery of stratiform PGE mineralization in the SLI and the DLS reinforces the suggestion (Neilsen and Brooks, 1995) that PGE reefs in tholeiitic layered intrusions constitute an important new type of mineral deposit. With world-wide demand for PGEs expected to increase steadily over the coming years, it is certain that tholeiitic layered intrusions will become active targets for exploration activity. Based on the PGE concentrations reported for the SLI, such activity should clearly include areas of northeastern Minnesota that have heretofore received little attention.

REFERENCES

Andersen, J. C. Ø., Rasmussen, H., Neilsen, T. F. D., Rønsbo, J. G., 1998, The Triple Group and the Platinova gold and palladium reefs in the Skaergaard Intrusion—stratigraphic and petrographic relations: Economic Geology, v. 93, p. 488–509.

Aranson, J. G., Bird, D. K., Bernstein, S., and Kelemen, P. B., 1997, Gold and platinum-group element mineralization in the Kruuse Fjord Gabbro complex, East Greenland: Economic Geology, v. 92, p. 490–501.

Barnes, S. J., and Campbell, I. H., 1988, Role of late magmatic fluids on Merensky-type platinum deposits: Geology, v. 16, p. 488–491.

Barnes, S-J., Couture, J-F., Sawyer, E. W., Bouchaib, C., 1993, Nickel-copper occurrences in the Belleterre-Angliers belt of the Pontiac Subprovince and the use of Cu-Pd ratios in interpreting platinum-group element distributions: Economic Geology, v. 88, p. 1402–1418.

Bird, D. K., Brooks, C. K., Gannicott, R. A., Turner, P. A., 1991, A gold-bearing horizon in the Skaergaard Intrusion, East Greenland: Economic Geology, v. 86, p. 1083–1092.

Bird, D. K., Aranson, J. G., Brandriss, M. E., Nevle, R. J., Radford, G., Bernstein, S., Gannicott, R. A., and Kelemen, P. B., 1995, A gold-bearing horizon in the Kap Edvard Holm Complex, East Greenland: Economic Geology, v. 90, p. 1288–1300.

Boerboom, T. J., and Miller, J. D., Jr., 1994, Geologic map of the Wilson Lake quadrangle and parts of the Silver Island Lake and Toohey Lake quadrangles, Lake and Cook Counties, Minnesota: Minnesota Geological Survey Miscellaneous Map Series M-81, scale 1:24,000.

Boudreau, A. E., and McCallum, I. S., 1992, Concentration of platinum-group elements by magmatic fluids in layered intrusions: Economic Geology, v. 87, p. 1830–1848.

Hauck, S. A., Severson, M. J., Zanko, L., Barnes, S. J., Morton, P., Aliminas, H., Foord, E. E., and Dahlberg, E. H., 1997, An overview of the geology and oxide, sulfide, platinum-group element mineralization along the western and northern contacts of the Duluth Complex *in* Ojakangas, R. J., Dickas, A. B., Green, J. C., eds., Middle Proterozoic and Cambrian Rifting, Central North America: Boulder, Colorado, Geological Society of America Special Paper 312, p. 137–185.

Hauck, S. A., Severson, M., Ripley, E., Goldberg, S., Alapieti, T., 1997, Geology and Cr-PGE mineralization of the Birch Lake area, South Kawishiwi Intrusion, Duluth Complex: Natural Resources Research Institute, University of Minnesota—Duluth, Technical Report NRRI/TR-97/13, 32 p.

Marsh, B. D., 1988, Crystal capture, sorting, and retention in convecting magma: Geological Society of America Bulletin, v. 100, p. 1720–1737.

Meints, J. P., Jirsa, M. A., Chandler, V. W., and Miller, J. D., Jr., 1993, Scientific core drilling in parts of Itasca, St. Louis, and Lake Counties, northeastern Minnesota: Minnesota Geological Survey Information Circular 37, 159 p.

Miller, J. D., Jr., 1995, Prediction and discovery of PGE occurrences in the Duluth Complex at Duluth [abs.]: 41st Annual Institute on Lake Superior Geology, p. 45-46.

Miller, J. D., Jr., 1998a, Potential for stratiform PGE deposits in sulfide-undersaturated, tholeiitic layered intrusions of the Duluth Complex, Minnesota, USA [abs.]: 8th International Platinum Symposium, Rustenburg, South Africa, GSSA and SAIMM Symposium Series S18, p. 263–266.

Miller, J. D., Jr., 1998b, Potential for reef-type PGE mineralization in the Duluth Complex: Evidence from the Layered Series at Duluth: The Minnesota Prospector, Special Issue, p. 8–12.

Miller, J. D., Jr., Boerboom, T. J., and Jerde, E. A., 1994, Geologic map of the Cabin Lake and Cramer quadrangles, Lake County, Minnesota: Minnesota Geological Survey Miscellaneous Map Series M-82, scale 1:24,000.

Miller, J. D., Jr., and Chandler, V. W., 1997, Geology, petrology, and tectonic significance of the Beaver Bay Complex, northeastern Minnesota *in* Ojakangas, R. J., Dickas, A. B., Green, J. C., eds., Middle Proterozoic and Cambrian Rifting, Central North America: Geological Society of America Special Paper 312, p. 73–96.

Miller, J. D., Jr., and Chandler, V. W., 1999, Bedrock geologic map of the central Duluth Complex and western part of the Beaver Bay Complex, Lake and St. Louis Counties, Minnesota: Minnesota Geological Survey Miscellaneous Map Series M-101, scale 1:100,000.

Miller, J. D. Jr., Green, J. C., Chandler, V. W., and Boerboom, T. J., 1993, Geologic map of the Finland and Doyle Lake quadrangles, Lake County, Minnesota: Minnesota Geological Survey Miscellaneous Map Series M-72, scale 1:24,000.

Miller, J. D., Jr., and Ripley, E. M., 1996, Layered intrusions of the Duluth Complex, Minnesota, USA *in* Cawthorne, R. G., ed., Layered Intrusions: Elsevier Scientific, Amsterdam, p. 257–301.

Naldrett, A. J., 1997, Key factors in the genesis of Noril'sk, Sudbury, Jinchuan, Voisey's Bay, and other world class Ni-Cu-PGE deposits: implications for exploration: Australian Journal of Earth Sciences, v. 44, p. 283–315.

Naldrett, A. J., 1993, Models for the formation of stata-bound concentrations of platinum-group elements in layered intrusions *in* Kirkham, R. V., Sinclair, W. D., Thorpe, R. I., Duke, J. M., eds., Mineral deposit modelling: Geological Association of Canada Special Paper, v. 40, p. 373–387.

Neilsen, T. F. D., and Brooks, C. K., 1995, Precious metals in magmas of East Greenland—Factors important to the mineralization in the Skaergaard Intrusion: Economic Geology, v. 90, p. 1911–1917.

Paces, J. B., and Miller, J. D., Jr., 1993, Precise U-Pb ages of Duluth Complex and related mafic intrusions, northeastern Minnesota—new insights for physical, petrogenetic, paleomagnetic and tectono-magmatic processes associated with 1.1 Ga Midcontinent rifting: Journal of Geophysical Research, v. 98, p. 13,997–14,013.

Rogge, M. K., 1989, Geochemistry of the Sonju Lake layered mafic intrusion: Ames, Iowa State University, unpublished M.A. thesis, 92 p.

Severson, M. J., 1998, Igneous stratigraphy and mineralization along the western margin of the Duluth Complex: The Minnesota Prospector, Special Issue, p. 13–15.

Stevenson, R. J., 1974, A mafic layered intrusion of Keweenawan age near Finland, Lake County, Minnesota: Duluth, University of Minnesota, unpublished M.S. thesis, 160 p.

APPENDIX

The analytical data presented in these tables were collected by Activation Laboratories Ltd. in Ancaster, Ontario, Canada. Analytical results for outcrop and drill-core samples from the already existing Minnesota Geological Survey collections are presented in Appendix Tables 2, 3, 4, and 5. Where adequate geochemical analyses already existed for these samples, partial analyses that included the desired elements were obtained , and were integrated with pre-existing data (Table 1, main text). Analytical results for the newly-collected outcrop samples from the favorable zone are presented in Appendix Tables 6, 7, 8, and 9.

The analytical technique, sample size and type, detection limits, and date of analysis are listed in each appendix table. Samples from the preexisting MGS collection are derived from various sources (see Table 2 in main text, and Appendix Table 1). Note that some of the results listed in Table 1 in the main text include data from earlier analyses. The newly collected outcrop samples from the favorable zone are numbered SLP-1 through SLP-17. The position of each of these samples within the Sonju Lake intrusion is shown in Table 1 and Figure 2B in the main text, and their UTM cordinates are given in Table 3 in the main text.

Appendix Table 1. Source of samples for which analytical data are presented

Sample Prefix	Source of sample
D, E and F	Outcrop samples collected by Minnesota Geological Survey between 1987 and 1990 during field mapping for COGEOMAP project
HS	Outcrop samples collected in 1993 by H. Staynov (University of Minnesota, Minneapolis) during field reconnaissance
WSL	Outcrop samples collected in 1998 by K. Wirth (Macalester College, St. Paul) for petrology teaching collection
SL	Outcrop samples collected in 1987 by M. K. Rogge (Iowa State University) for MS thesis (Rogge, 1989)
SLI	Samples from drill core SLI-1 drilled in 1991 for Minnesota Geological Survey as part of the central Duluth Complex drilling project. Currently in temporary storage at the Minnesota Geological Survey
SNWR	Outcrop samples collected in 1982 by J. Beck (E. K. Lehmann and Associates) during exploration activities
SNA	Samples from drill core SNA-1 drilled in 1982 for E. K. Lehman and Associates; Now in storage at Department of Natural Resources (DNR) Minerals Division in Hibbing, Minnesota
SLP	Outcrop samples collected from two traverses across the favorable horizon (Fig. 2B) for this study

Appendix Table 2. INAA analyses completed by Activation Laboratories Ltd., Ancaster, Ontario, Canada, April 12, 1999

[units of measurement and detection limits shown at top of each column; for each analysis, 30g of powdered sample was encapsulated, irradiated, and measured in a multielement mode by Instrumental Neutron Activation Analysis]

Sample	Au	Ag	As	Ba	Br	Co	Cr	Cs	Fe	Hf	Hg
Unit of meas.	ppb	ppm	ppm	ppm	ppm	ppm	ppm	ppm	%	ppm	ppm
Detect. limit.	2	5	0.5	50	0.5	1	5	1	0.01	1	1
D281	<2	<5	<0.5	<50	<0.5	65	96	1	9.74	1	<1
D288	<2	<5	0.9	170	<0.5	75	343	<1	9.53	2	<1
D301A	<2	<5	1.1	270	1.9	79	291	<1	9.40	2	<1
D301B	<2	<5	<0.5	160	<0.5	72	405	<1	7.89	<1	<1
E250	7	<5	1.9	1100	<0.5	4	62	2	8.21	15	<1
F295	4	<5	<0.5	150	<0.5	87	395	<1	12.40	1	<1
F300A	<2	<5	1.3	230	<0.5	35	310	<1	6.46	2	<1
F319	10	<5	3.0	520	<0.5	35	6	3	16.40	5	<1
F322A	<2	<5	<0.5	290	<0.5	46	<5	<1	12.50	4	<1
F322C	12	<5	<0.5	<52	<0.5	46	<5	<1	15.00	3	<1
F322L	<2	<5	1.7	390	<0.5	45	<5	3	11.90	4	<1
F328	<2	<5	<0.5	<50	<0.5	28	<5	<1	5.96	2	<1
F330	17	<5	<0.5	250	<0.5	65	8	<1	12.90	2	<1
F332	<2	<5	<0.5	190	<0.5	81	<5	<1	15.30	2	<1
F334A	7	<5	2.4	230	<0.5	56	6	3	11.60	2	<1
F335	<2	<5	<0.5	<59	<0.5	66	<5	3	13.70	2	<1
F407A	<3	<5	<0.5	<62	4.5	147	<5	<1	30.40	3	<1
HS14A	4	<5	<0.5	340	<0.5	72	150	<1	14.60	2	<1
SNA 101.5	<2	<5	1.0	140	3.0	88	94	<1	9.15	1	<1
SNA 198	4	<5	1.2	<50	7.0	96	51	<1	8.43	<1	<1
SNA 276	<2	<5	<0.5	<50	12.4	154	121	<1	11.90	<1	<1
WSL6	<2	<5	<0.5	<50	2.1	76	157	1	8.69	<1	<1
WSL9	<2	<5	<0.5	<50	<0.5	62	268	<1	7.11	<1	<1
WSL10	<2	<5	<0.5	210	<0.5	55	449	<1	8.30	2	<1
WSL11	<2	<5	<0.5	140	1.5	61	323	<1	8.07	2	<1
WSL12	4	<5	<0.5	160	<0.5	76	392	1	9.60	2	<1
WSL14	<2	<5	<0.5	240	<0.5	72	51	<1	13.40	<1	<1
WSL15	<2	<5	<0.5	340	2.4	43	9	<1	9.26	3	<1
WSL19	<2	<5	<0.5	<50	<0.5	30	8	<1	6.68	1	<1
WSL20	<2	<5	<0.5	<50	<0.5	70	<5	<1	13.40	2	<1

Appendix Table 2. ctd...

Sample	Ir	Mo	Na	Rb	Sb	Sc	Se	Sn	Sr	Ta	Th
Unit of meas.	ppb	ppm	%	ppm	ppm	ppm	ppm	%	%	ppm	ppm
Detect. limit	5	1	0.01	15	0.1	0.1	3	0.01	0.05	0.5	0.2
D281	<5	<1	1.88	<15	0.1	20.4	<3	<0.01	<0.05	<0.5	1.4
D288	<5	<1	2.13	<15	0.3	14.6	<3	<0.01	<0.05	<0.5	<0.2
D301A	<5	<1	1.90	<15	0.3	7.8	<3	<0.01	<0.05	1.3	1.2
D301B	<5	<1	2.01	<15	0.2	8.7	<3	<0.01	<0.05	<0.5	0.3
E250	<5	<1	2.85	79	0.2	8.4	<3	<0.01	<0.05	2.8	9.4
F295	<5	<1	1.74	<15	<0.1	49.9	<3	<0.02	<0.05	<0.5	1.6
F300A	<5	<1	2.52	<15	<0.1	28.4	<3	<0.01	<0.05	1.6	<0.2
F319	<5	1	2.21	<15	<0.1	41.4	<3	<0.02	<0.05	1.0	3.4
F322A	<5	<1	2.27	<15	<0.1	53.4	<3	<0.02	<0.05	0.7	1.8
F322C	<5	<1	1.92	<15	<0.1	55.0	<3	<0.02	<0.05	1.5	1.4
F322L	<5	<1	2.45	45	0.3	17.8	<3	<0.01	<0.05	1.6	2.2
F328	<5	<1	2.97	<15	<0.1	11.2	<3	<0.01	<0.05	<0.5	1.1
F330	<5	<1	2.58	<15	1.5	41.0	<3	<0.02	<0.05	<0.5	1.2
F332	<5	<1	2.00	<15	<0.1	47.4	<3	<0.02	<0.05	<0.5	0.6
F334A	<5	<1	2.04	<15	0.2	45.7	<3	<0.02	<0.05	<0.5	1.2
F335	<5	<1	1.97	<15	<0.1	61.7	<3	<0.02	<0.05	<0.5	1.1
F407A	<5	<1	0.38	<15	<0.1	64.0	<3	<0.02	<0.05	<0.5	<0.2
HS14A	<5	<1	1.61	<15	<0.1	62.1	<3	<0.02	<0.05	1.5	1.0
SNA 101.5	<5	<1	1.30	<15	0.4	14.1	<3	<0.01	<0.05	<0.5	<0.2
SNA 198	<5	<1	1.12	<15	0.2	5.2	<3	<0.01	<0.05	<0.5	0.3
SNA 276	<5	<1	0.32	<15	<0.1	8.3	<3	<0.01	<0.05	<0.5	<0.2
WSL6	<5	<1	1.67	<15	<0.1	9.4	<3	<0.01	<0.05	<0.5	<0.2
WSL9	<5	<1	1.98	<15	0.4	12.8	<3	<0.01	<0.05	<0.5	<0.2
WSL10	<5	<1	2.08	22	<0.1	36.1	<3	<0.02	<0.05	<0.5	1.4
WSL11	<5	<1	2.20	<15	<0.1	13.8	<3	<0.01	<0.05	<0.5	<0.2
WSL12	<5	<1	2.09	26	<0.1	17.2	<3	<0.01	<0.05	<0.5	1.0
WSL14	<5	<1	1.50	<15	<0.1	65.3	<3	<0.02	<0.05	<0.5	1.0
WSL15	<5	<1	2.53	37	<0.1	37.3	<3	<0.02	<0.05	<0.5	1.9
WSL19	<5	<1	2.66	<15	0.3	25.7	<3	<0.01	<0.05	<0.5	1.4
WSL20	<5	<1	1.77	<15	<0.1	48.6	<3	<0.02	<0.05	<0.5	0.7

Appendix Table 2. ctd...

Sample	U	W	Zn	La	Ce	Nd	Sm	Eu	Tb	Yb	Lu
Unit of mes.	ppm	ppm	ppm	ppm	ppm	ppm	ppm	ppm	ppm	ppm	ppm
Detect. limit	0.5	1	50	0.5	3	5	0.1	0.2	0.5	0.2	0.05
D281	1.3	<1	124	7.5	16	8	2.2	0.9	<0.5	1.1	0.24
D288	<0.5	<1	<50	7.7	13	7	2.1	0.8	<0.5	1.0	0.21
D301A	<0.5	<1	71	10.2	19	10	2.7	0.9	<0.5	1.1	0.20
D301B	<0.5	<1	83	2.1	5	<5	0.6	0.6	<0.5	0.3	0.05
E250	2.9	<1	188	72.9	128	58	17.2	5.9	2.7	11.5	1.65
F295	<0.5	<1	195	8.8	20	13	3.1	1.0	0.8	2.1	0.36
F300A	<0.5	<1	<50	8.8	16	13	2.5	0.9	<0.5	1.4	0.24
F319	<0.5	<1	208	48.4	95	46	14.7	4.0	1.8	6.0	0.98
F322A	<0.5	<1	257	16.3	33	26	5.0	2.0	0.9	2.5	0.41
F322C	<0.5	<1	235	26.4	53	33	10.0	3.3	1.1	3.5	0.58
F322L	1.4	<1	98	16.3	29	14	3.1	2.0	0.7	1.5	0.27
F328	<0.5	<1	<50	9.4	14	12	2.2	1.1	0.7	1.2	0.19
F330	<0.5	<1	136	11.2	21	17	3.0	1.3	<0.5	1.8	0.30
F332	<0.5	<1	88	7.9	14	7	2.4	1.1	0.6	1.6	0.20
F334A	<0.5	<1	147	9.6	18	13	2.9	1.3	<0.5	1.6	0.33
F335	<0.5	<1	<50	7.8	11	13	2.9	1.0	<0.5	1.9	0.23
F407A	<0.5	<1	442	3.2	6	<5	1.4	0.7	<0.5	1.1	0.20
HS14A	<0.5	<1	183	6.5	14	6	2.3	0.9	<0.5	1.6	0.27
SNA101.5	<0.5	<1	<50	6.4	14	6	2.0	0.8	<0.5	1.0	0.17
SNA 198	<0.5	<1	80	2.1	6	<5	0.5	0.4	<0.5	0.3	<0.05
SNA 276	<0.5	<1	113	0.7	<3	<5	0.2	0.2	<0.5	0.3	<0.05
WSL6	<0.5	<1	71	4.1	8	<5	1.2	0.6	<0.5	0.6	0.11
WSL9	<0.5	<1	<50	4.1	8	<5	1.2	0.6	<0.5	0.7	0.14
WSL10	<0.5	<1	143	9.3	18	12	2.7	1.0	0.9	1.6	0.22
WSL11	<0.5	<1	59	8.4	17	9	2.2	0.9	<0.5	1.1	0.25
WSL12	1.4	<1	78	8.6	12	6	2.3	0.8	<0.5	1.1	0.28
WSL14	<0.5	<1	172	6.8	13	6	2.4	0.8	<0.5	1.5	0.20
WSL15	<0.5	<1	130	13.4	26	14	3.7	1.6	0.8	1.8	0.34
WSL19	<0.5	<1	171	7.6	13	7	2.1	0.9	<0.5	1.1	0.18
WSL20	<0.5	<1	<50	9.3	17	11	2.9	1.1	<0.5	1.7	0.28

Appendix Table 3. ICP-MS analyses completed by Activation Laboratories Ltd., Ancaster, Ontario, Canada, April 12, 1999

[units of measurement and detection limits shown at top of each column; 30g of powdered sample was digested using HF, $HCLO_4$, HNO, and HCL; metal concentrations determined by inductively coupled plasma emission mass spectrometry; aluminium may not be total; phases that may not be totally digested include zircon, monazite, sphene, gahnite, chromite, magnetite, barite, cassiterite, ilmenite and rutile]

Sample	Mo	Cu	Pb	Zn	Ag	Ni	Mn	Sr	Cd	Bi
Unit of meas.	ppm	ppm	ppm	ppm	ppm	ppm	ppm	ppm	ppm	ppm
Detect. limit	2	1	5	1	0.4	1	1	1	0.5	5
D281	<2	97	<5	95	0.5	201	1210	348	1.3	<5
D287	<2	47	<5	71	<0.4	168	1181	279	<0.5	<5
D288	<2	62	<5	81	0.4	242	1157	362	0.6	<5
D301A	<2	101	<5	91	0.5	327	1139	367	0.8	<5
D301B	<2	29	<5	68	<0.4	396	937	384	0.5	<5
E246	3	37	14	215	1.4	2	1972	245	0.7	<5
E250	3	17	14	156	2.7	2	1554	259	<0.5	<5
F140	2	13	22	119	2.4	2	416	44	<0.5	<5
F229	<2	432	6	142	0.9	2	1824	271	1.8	<5
F231	<2	57	<5	175	0.5	112	2334	72	5.7	<5
F295	<2	65	<5	97	0.4	166	1585	242	1.7	<5
F300A	<2	61	<5	60	0.6	63	919	398	0.8	<5
F311	<2	168	<5	133	1.3	2	2042	316	1.5	<5
F312	<2	304	<5	171	1.3	3	2121	267	2.0	<5
F319	2	107	<5	216	1.4	2	2659	327	3.9	<5
F322A	<2	371	<5	120	1.1	2	1750	353	2.1	<5
F322C	<2	367	<5	139	1.1	2	2262	309	2.9	<5
F322L	<2	223	<5	101	1.0	2	1090	594	2.2	<5
F325	2	46	9	220	2.2	2	2287	244	0.8	<5
F328	<2	79	<5	66	0.6	16	796	492	<0.5	<5
F330	<2	630	5	96	1.1	9	1321	382	1.9	<5
F332	<2	71	<5	124	0.7	63	1463	288	2.5	<5
F334A	<2	85	<5	92	0.8	32	1167	324	1.7	<5
F335	<2	46	<5	98	0.6	64	1424	262	2.2	<5
F395R	<2	96	<5	67	0.7	10	829	396	0.7	<5
F407A	<2	1865	5	270	1.1	12	2358	61	12.6	8
F411	<2	72	<5	101	0.7	15	1354	243	1.4	<5
HS14A	<2	60	<5	108	0.6	132	1419	261	2.9	<5
SLI 242	2	66	6	171	1.5	2	2389	241	2.4	<5
SLI 242-re[1]	2	66	6	169	1.5	2	2466	248	2.1	<5
SLI 318	3	77	5	184	1.1	2	2782	259	2.8	<5
SLI 457	2	60	6	161	1.7	2	2104	266	1.6	<5
SLI 586	2	50	<5	137	1.0	6	2244	211	2.0	<5
SLI 830	2	76	<5	187	1.2	13	2285	290	2.5	<5
SNA 101.5	<2	85	<5	73	<0.4	494	1180	397	0.8	<5
SNA 198	<2	26	<5	71	<0.4	731	1088	350	0.7	<5
SNA 276	<2	29	<5	97	<0.4	1306	1500	209	1.4	<5
SNA 310	<2	57	<5	93	<0.4	1278	1662	7	0.5	<5
SNA 340	<2	5	8	64	<0.4	953	1360	341	<0.5	<5
SNA 492	<2	12	5	54	<0.4	858	904	221	<0.5	<5
SNA 554	<2	12	<5	59	<0.4	971	887	255	<0.5	<5
WSL6	<2	64	<5	82	<0.4	334	1053	385	0.7	<5
WSL9	<2	29	<5	66	<0.4	245	947	376	1.1	<5
WSL10	<2	75	<5	76	0.6	123	1174	325	0.5	<5
WSL11	<2	68	<5	78	0.5	184	1084	415	<0.5	<5
WSL12	<2	67	<5	89	0.5	180	1247	352	0.6	<5
WSL14	<2	54	<5	96	0.6	122	1393	210	2.7	<5
WSL15	<2	406	<5	91	1.3	2	1044	380	1.1	<5
WSL19	<2	60	<5	74	0.5	18	814	414	1.4	<5
WSL20	<2	97	<5	113	0.9	55	1542	277	2.6	<5

[1]repeat analysis

Appendix Table 3. ctd...

Sample	V	Ca	P	Mg	Ti	Al	K	Y	Be	S
Unit of meas.	ppm	%	%	%	%	%	%	ppm	ppm	%
Detect. limit	2	0.01	0.001	0.01	0.01	0.01	0.01	2	2	0.01
D281	174	6.87	0.024	4.29	0.71	8.26	0.40	7	<2	0.05
D287	140	7.43	0.009	4.98	0.45	7.54	0.29	7	<2	0.06
D288	106	6.93	0.027	5.20	0.47	9.06	0.41	7	<2	0.05
D301A	104	6.46	0.044	5.43	0.53	9.14	0.37	9	<2	0.05
D301B	62	7.22	0.002	5.45	0.23	9.91	0.24	2	<2	0.05
E246	8	3.08	0.128	0.40	0.90	5.55	2.56	66	3	0.08
E250	3	2.50	0.051	0.21	0.48	6.18	3.10	77	3	0.04
F140	4	0.15	0.003	0.02	0.14	5.94	4.08	69	5	0.01
F229	77	6.58	0.038	2.50	1.65	5.59	0.47	8	<2	0.08
F231	1014	5.50	0.008	6.36	1.66	2.29	0.12	3	<2	0.04
F295	208	7.80	0.027	5.93	0.61	6.14	0.39	11	<2	0.05
F300A	205	8.40	0.028	2.80	0.67	9.73	0.42	10	<2	0.06
F311	31	5.57	0.352	1.66	1.56	6.38	0.76	24	<2	0.13
F312	94	5.37	0.123	1.85	1.64	5.46	0.86	24	<2	0.07
F319	30	6.50	0.534	1.50	1.78	5.82	1.02	44	<2	0.21
F322A	73	7.44	0.069	2.31	1.88	6.65	0.97	14	<2	0.05
F322C	48	8.29	0.647	2.47	1.88	5.41	0.65	28	<2	0.07
F322L	151	3.67	0.059	0.75	1.88	8.50	1.84	2	<2	0.03
F325	11	3.30	0.261	0.90	1.17	5.30	1.77	52	2	0.04
F328	152	7.57	0.027	1.51	0.68	11.44	0.62	9	<2	0.05
F330	434	7.35	0.033	2.91	1.90	8.25	0.53	4	<2	0.05
F332	796	7.62	0.020	3.81	1.77	7.06	0.36	6	<2	0.05
F334A	686	8.42	0.026	2.84	1.74	8.21	0.49	7	<2	0.05
F335	735	8.49	0.018	3.78	1.45	6.59	0.38	8	<2	0.06
F395R	229	6.74	0.042	1.26	0.95	9.85	0.58	10	<2	0.06
F407A	387	4.97	0.005	3.19	1.89	1.81	0.08	2	<2	0.09
F411	466	6.88	0.028	3.08	1.66	6.39	0.40	7	<2	0.05
HS14A	1069	9.19	0.020	4.21	1.81	6.59	0.30	7	<2	0.06
SLI 242	24	5.12	0.369	1.45	1.53	4.63	1.17	40	<2	0.24
SLI 242-re[1]	24	5.21	0.369	1.49	1.56	4.78	1.22	40	<2	0.22
SLI 318	31	5.28	0.426	1.23	1.55	4.58	0.92	35	<2	0.21
SLI 457	41	4.79	0.369	1.13	1.34	5.22	1.33	45	2	0.17
SLI 586	110	6.58	0.681	2.09	1.62	4.01	0.81	41	<2	0.10
SLI 830	124	5.54	0.391	1.72	1.63	5.35	0.89	32	<2	0.19
SNA 101.5	86	7.44	0.029	6.95	0.49	8.65	0.27	7	<2	0.05
SNA 198	25	6.96	0.008	8.19	0.16	8.97	0.11	2	<2	0.05
SNA 276	19	3.11	0.002	11.70	0.07	3.90	0.08	2	<2	0.03
SNA 310	47	0.22	0.032	13.40	0.21	1.09	0.08	3	<2	0.05
SNA 340	14	1.46	0.002	11.17	0.04	4.42	0.07	2	<2	0.03
SNA 492	15	5.25	0.002	8.87	0.06	7.25	0.05	2	<2	0.05
SNA 554	13	5.20	0.002	8.89	0.05	7.49	0.05	2	<2	0.04
WSL6	101	7.31	0.016	5.49	0.45	9.67	0.26	3	<2	0.05
WSL9	77	7.36	0.008	4.86	0.37	9.76	0.28	3	<2	0.05
WSL10	182	8.35	0.034	4.56	0.65	8.21	0.48	11	<2	0.06
WSL11	116	7.27	0.026	4.42	0.60	9.95	0.53	8	<2	0.05
WSL12	132	6.99	0.027	5.13	0.56	8.85	0.46	8	<2	0.05
WSL14	949	8.75	0.020	4.24	1.53	5.66	0.30	8	<2	0.06
WSL15	276	7.02	0.044	1.99	1.82	8.13	0.62	8	<2	0.07
WSL19	384	7.69	0.027	1.67	0.94	9.52	0.48	8	<2	0.06
WSL20	779	8.17	0.037	3.79	1.79	6.82	0.44	9	<2	0.05

[1]repeat analysis

Appendix Table 4. Assay analyses completed by Activation Laboratories Ltd., Ancaster, Ontario, Canada, April 12, 1999

[fire assay sample analyzed by inductively coupled plasma emission mass spectrometry; measured in parts per billion; detection limits shown at top of each column]

Sample	Sample wt. (grams)	Pd	Pt	Au
Unit of meas.		ppb	ppb	ppb
Detect. limit		0.1	0.1	1
D281	30	0.4	<0.1	30
D287	15	3.9	0.4	<2
D288	30	1.9	<0.1	2
D301A	30	3.1	0.1	123
D301B	30	1.1	<0.1	2
E250	30	<0.1	<0.1	3
F140	30	0.2	0.6	<1
F229	30	<0.1	<0.1	1
F231	30	5.1	12	5
F295	30	1.9	<0.1	6
F300A	30	2.0	<0.1	1
F311	30	<0.1	<0.1	2
F312	30	<0.1	<0.1	5
F319	30	<0.1	<0.1	3
F322A	30	<0.1	<0.1	<1
F322C	30	<0.1	<0.1	20
F322L	30	<0.1	<0.1	3
F325	30	<0.1	<0.1	4
F328	30	16	23	3
F330	30	0.3	<0.1	27
F332	30	6.8	5.6	1
F334A	30	36	2.6	3
F395R	30	17	22	2
F411	30	320	66	6
F470A	30	<0.1	<0.1	3
HS14A	30	3.5	<0.1	2
SLI242	30	1.1	<0.1	3
SLI318	30	<0.1	<0.1	3
SLI457	30	<0.1	<0.1	3
SLI586	30	<0.1	<0.1	<1
SLI830	30	0.2	<0.1	<1
SNA 101.5	30	0.8	<0.1	2
SNA 198	30	0.7	<0.1	1
SNA 276	30	2.1	<0.1	<1
SNA 310	30	0.7	<0.1	3
SNA 340	30	<0.1	<0.1	5
SNA492	30	0.2	<0.1	5
WSL6	30	1.2	<0.1	1
WSL9	30	0.8	<0.1	<1
WSL10	30	1.8	<0.1	3
WSL11	30	2.0	<0.1	2
WSL12	30	2.1	<0.1	1
WSL14	30	1.0	<0.1	<1
WSL15	30	0.5	<0.1	2
WSL19	30	17	25	6
WSL20	30	4.6	6.8	<1

Appendix Table 5. XRF sulfur analyses completed by Activation Laboratories, Ancaster, Ontario, Canada, April 12, and July 30, 1999

[analyzed by X-ray flourescence of 6 gm pressed powder pellet; measured in parts per million; detection limit is 50 ppm; –, not analyzed on date indicated]

Sample	S	S
Date	13-May-99	30-July-99
D287	<50	–
D301A	–	214
E234A	360	–
E246	780	–
E250	–	241
F140	<50	–
F229	540	–
F231	<50	–
F300A	–	115
F311	1595	–
F312	650	–
F322C	–	403
F322L	–	134
F325	105	–
F395R	<50	–
F411	<50	–
SLI 242	3150	–
SLI 318	2860	–
SLI 457	1910	–
SLI 586	1055	–
SLI 830	2550	–
SNA 101.5	–	289
SNA 198	–	287
SNA 276	–	194
SNA 310	405	–
SNA 340	145	–
SNA 492	100	–
SNA 554	550	–
WSL6	–	267
WSL9	–	202
WSL10	–	96
WSL11	–	269
WSL12	–	129
WSL14	–	76
WSL15	–	375
WSL19	–	199
WSL20	–	192

Appendix Table 6. INAA analyses completed by Activation Laboratories, Ancaster, Ontario, Canada, June 29, 1999

[units of measurement and detection limits shown at top of each column; for each analysis, 30g of powdered sample was encapsulated, irradiated, and measured in a multielement mode by Instrumental Neutron Activation Analysis]

Sample	Au	Ag	As	Ba	Br	Co	Cr	Cs	Fe	Hf	Hg
Unit meas.	ppb	ppm	ppm	ppm	ppm	ppm	ppm	ppm	%	ppm	ppm
Detect. limit	2	5	0.5	50	0.5	1	5	1	0.01	1	1
SLP-1	13	<5	<0.5	300	<0.5	50	<5	1	9.93	2	<1
SLP-2	<2	<5	<0.5	190	<0.5	43	<5	<1	9.09	2	<1
SLP-3	<2	<5	<0.5	140	<0.5	44	<5	1	8.99	2	<1
SLP-4	<2	<5	<0.5	140	<0.5	58	<5	<1	10.8	2	<1
SLP-5	27	<5	<0.5	310	<0.5	76	<5	1	13.0	2	<1
SLP-6	<2	<5	<0.5	150	<0.5	54	<5	<1	9.64	2	<1
SLP-7	<2	<5	<0.5	100	<0.5	68	<5	<1	12.3	2	<1
SLP-8	<2	<5	<0.5	130	<0.5	59	<5	3	11.1	2	<1
SLP-9	<2	<5	<0.5	340	<0.5	56	<5	<1	10.8	2	<1
SLP-10	<2	<5	<0.5	120	<0.5	87	<5	2	14.7	2	<1
SLP-11	<2	<5	<0.5	150	<0.5	35	<5	2	7.53	2	<1
SLP-12	<2	<5	<0.5	260	<0.5	41	<5	<1	7.90	3	<1
SLP-13	<2	<5	<0.5	130	<0.5	58	<5	<1	10.0	3	<1
SLP-14	<2	<5	<0.5	300	<0.5	28	<5	1	5.34	2	<1
SLP-15	<2	<5	<0.5	100	<0.5	41	<5	<1	7.08	2	<1
SLP-16	8	<5	<0.5	110	<0.5	40	<5	<1	7.92	2	<1
SLP-17	<2	<5	<0.5	100	<0.5	55	<5	2	9.49	2	<1

Appendix Table 6. ctd...

Sample	Ir	Mo	Na	Rb	Sb	Sc	Se	Sn	Sr	Ta	Th
Unit meas.	ppb	ppm	%	ppm	ppm	ppm	ppm	%	%	ppm	ppm
Detect. limit	5	1	0.01	15	0.1	0.1	3	0.01	0.05	0.5	0.2
SLP-1	<5	<1	2.36	<15	<0.1	40.7	<3	<0.02	<0.05	<0.5	0.9
SLP-2	<5	<1	2.56	<15	<0.1	34.5	<3	<0.01	<0.05	<0.5	0.9
SLP-3	<5	<1	2.39	<15	<0.1	41.7	<3	<0.02	<0.05	<0.5	1.3
SLP-4	<5	<1	2.14	<15	<0.1	36.2	<3	<0.01	<0.05	<0.5	<0.2
SLP-5	<5	<1	1.90	<15	<0.1	46.1	<3	<0.02	<0.05	<0.5	1.2
SLP-6	<5	<1	2.27	<15	<0.1	39.9	<3	<0.02	<0.05	<0.5	1.1
SLP-7	<5	<1	1.68	40	<0.1	57.0	<3	<0.02	<0.05	<0.5	1.4
SLP-8	<5	<1	1.89	<15	<0.1	43.9	<3	<0.01	<0.05	<0.5	1.1
SLP-9	<5	<1	2.17	<15	<0.1	40.7	<3	<0.01	<0.05	<0.5	1.4
SLP-10	<5	<1	1.90	<15	<0.1	34.8	<3	<0.01	<0.05	<0.5	1.2
SLP-11	<5	<1	2.52	<15	<0.1	28.0	<3	<0.01	<0.05	<0.5	0.5
SLP-12	<5	<1	2.57	<15	<0.1	34.9	<3	<0.02	<0.05	<0.5	1.7
SLP-13	<5	<1	2.39	<15	<0.1	34.1	<3	<0.02	<0.05	2.5	0.8
SLP-14	<5	<1	2.82	<15	<0.1	12.6	<3	<0.01	<0.05	<0.5	1.6
SLP-15	<5	<1	2.16	<15	<0.1	38.1	<3	<0.01	<0.05	2.2	<0.2
SLP-16	<5	<1	2.40	<15	<0.1	32.0	<3	<0.01	<0.05	<0.5	1.3
SLP-17	<5	<1	2.01	<15	0.4	47.9	<3	<0.01	<0.05	<0.5	<0.2

Appendix Table 6. ctd...

Sample	U	W	Zn	La	Ce	Nd	Sm	Eu	Tb	Yb	Lu
Unit meas.	ppm	ppm	ppm	ppm	ppm	ppm	ppm	ppm	ppm	ppm	ppm
Detect. limit	0.5	1	50	0.5	3	5	0.1	0.2	0.5	0.2	0.01
SLP-1	<0.5	<1	<50	9.9	19	<5	3.1	1.4	<0.5	1.7	0.25
SLP-2	<0.5	<1	<50	10.3	20	<5	3.0	1.3	<0.5	1.6	0.19
SLP-3	<0.5	<1	<50	9.6	19	13	3.0	1.4	<0.5	1.5	0.22
SLP-4	<0.5	<1	66	9.9	17	8	2.9	1.3	<0.5	1.4	0.26
SLP-5	<0.5	<1	<50	9.1	21	<5	2.9	1.2	<0.5	1.5	0.33
SLP-6	<0.5	<1	<50	10.3	22	15	3.0	1.3	<0.5	1.6	0.25
SLP-7	<0.5	<1	<50	9.5	19	10	3.5	1.3	0.7	1.9	0.32
SLP-8	<0.5	<1	<50	10.9	23	13	3.4	1.2	<0.5	1.8	0.27
SLP-9	<0.5	<1	<50	12.3	25	14	4.0	1.5	0.6	2.0	0.33
SLP-10	<0.5	<1	116	9.2	19	<5	2.8	1.2	<0.5	1.6	0.28
SLP-11	<0.5	<1	<50	10.8	20	12	3.2	1.4	<0.5	1.8	0.26
SLP-12	<0.5	<1	101	11.8	26	11	3.6	1.5	<0.5	2.2	0.36
SLP-13	<0.5	<1	<50	10.6	20	20	3.9	1.5	<0.5	2.0	0.35
SLP-14	<0.5	<1	<50	11.6	23	9	3.9	1.5	<0.5	1.6	0.31
SLP-15	<0.5	<1	<50	5.4	13	11	2.7	1.2	<0.5	1.4	0.21
SLP-16	<0.5	<1	<50	7.7	17	11	3.3	1.2	0.7	1.5	0.33
SLP-17	<0.5	<1	88	6.3	17	<5	3.0	1.1	<0.5	1.7	0.31

Appendix Table 7. ICP-MS analyses completed by Activation Laboratories Ltd., Ancaster, Ontario, Canada, June 25, 1999

[units of measurement and detection limits shown at top of each column; 30g of powdered sample was digested using HF, $HCLO_4$, HNO, and HCL; metal concentrations determined by inductively coupled plasma emission mass spectrometry; aluminium may not be total; phases that may not be totally digested include zircon, monazite, sphene, gahnite, chromite, magnetite, barite, cassiterite, ilmenite and rutile]

Sample	Mo	Cu	Pb	Zn	Ag	Ni	Mn	Sr	Cd	Bi
Unit meas.	ppm	ppm	ppm	ppm	ppm	ppm	ppm	ppm	ppm	ppm
Detect. limit	2	1	5	1	0.4	1	1	1	0.5	5
SLP-1	<2	515	<5	115	0.5	5	1190	292	5.1	<5
SLP-2	<2	473	<5	111	<0.4	4	1085	314	4.6	<5
SLP-3	<2	402	<5	116	<0.4	5	1094	300	4.9	<5
SLP-4	<2	618	<5	149	0.6	9	1281	270	6.9	<5
SLP-5	<2	514	<5	138	0.5	14	1428	224	7.7	<5
SLP-6	<2	82	<5	140	<0.4	13	1084	273	5.7	<5
SLP-7	<2	78	<5	136	<0.4	22	1284	185	8.4	<5
SLP-8	<2	78	<5	133	<0.4	34	1163	220	6.8	<5
SLP-9	<2	102	<5	127	<0.4	26	1130	264	6.7	<5
SLP-10	<2	80	<5	152	<0.4	59	1403	235	9.8	<5
SLP-11	<2	89	<5	126	<0.4	16	997	323	3.6	<5
SLP-12	<2	375	<5	107	<0.4	5	959	322	4.1	<5
SLP-13	<2	368	<5	117	<0.4	6	1154	284	6.1	<5
SLP-14	<2	30	<5	96	<0.4	6	618	374	3.0	<5
SLP-15	<2	37	<5	99	<0.4	23	863	276	4.1	<5
SLP-15r	<2	36	<5	95	<0.4	22	879	281	3.3	<5
SLP-16	<2	52	<5	110	<0.4	23	890	299	4.4	<5
SLP-17	<2	51	<5	118	0.5	41	1111	253	5.9	<5

Appendix Table 7. ctd...

Sample	V	Ca	P	Mg	Ti	Al	K	Y	Be	S
Unit meas.	ppm	%	%	%	%	%	%	ppm	ppm	%
Detect. limit	2	0.01	0.001	0.01	0.01	0.01	0.01	2	2	0.01
SLP-1	268	5.98	0.040	2.31	2.65	7.78	0.31	4	<2	0.10
SLP-2	213	5.77	0.040	2.03	2.52	8.29	0.46	6	<2	0.08
SLP-3	292	6.30	0.037	2.13	2.37	7.94	0.33	6	<2	0.08
SLP-4	371	5.36	0.042	2.52	2.97	7.30	0.40	2	<2	0.07
SLP-5	506	5.63	0.035	3.33	2.63	6.57	0.33	3	<2	0.07
SLP-6	419	6.03	0.044	2.23	2.48	7.86	0.44	4	<2	0.09
SLP-7	710	6.31	0.036	3.21	2.07	5.83	0.31	9	<2	0.09
SLP-8	636	6.05	0.040	2.75	1.78	6.74	0.35	9	<2	0.09
SLP-9	561	6.37	0.095	2.49	1.79	7.76	0.40	11	<2	0.09
SLP-10	811	5.23	0.034	3.39	2.16	6.82	0.37	4	<2	0.07
SLP-11	312	6.57	0.046	1.70	1.15	9.12	0.42	11	<2	0.09
SLP-12	247	6.08	0.048	1.75	1.96	8.28	0.40	8	<2	0.08
SLP-13	226	5.34	0.037	2.30	2.26	7.48	0.36	4	<2	0.07
SLP-14	133	5.66	0.046	1.15	1.23	9.88	0.56	7	<2	0.08
SLP-15	331	6.90	0.019	2.24	0.88	7.89	0.27	7	<2	0.11
SLP-15r	336	6.92	0.018	2.24	0.97	8.09	0.28	6	<2	0.10
SLP-16	443	6.64	0.026	1.83	1.11	8.62	0.34	7	<2	0.09
SLP-17	596	6.99	0.026	2.77	1.36	7.42	0.28	7	<2	0.10

Appendix Table 8. Assay analyses completed by Activation Laboratories Ltd., Ancaster, Ontario, Canada, June 25, 1999

[fire assay sample analyzed by inductively coupled plasma emission mass spectrometry; measured in parts per billion; detection limits shown at top of each column]

Sample	sample wt. (grams)	Pd	Pt	Au
Unit of meas.		ppb	ppb	ppb
Detect. limit		0.1	0.1	1
SLP-1	30	0.8	1.8	5
SLP-2	30	0.9	2.1	1
SLP-3	30	1.0	1.1	85
SLP-4	30	0.5	1.5	3
SLP-5	30	<0.1	6.0	12
SLP-6	30	179	40.4	1
SLP-7	30	293	50.9	1
SLP-8	30	19.1	4.8	<1
SLP-9	30	21.4	2.5	<1
SLP-10	30	7.0	11.8	2
SLP-11	30	5.7	3.1	<1
SLP-12	30	1.4	1.3	2
SLP-13	30	0.9	2.0	<1
SLP-14	30	133	4.6	1
SLP-15	30	6.5	15.5	<1
SLP-16	30	18.7	29.7	1
SLP-17	30	1.0	1.3	<1

Appendix Table 9. XRF sulfur analyses completed by Activation Laboratories Ltd., Ancaster, Ontario, Canada, August 11, 1999

[analyzed by X-ray flourescence of 6 gm pressed powder pellet; measured in parts per million; detection limit is 50 ppm]

Sample	S
unit meas.	ppm
Detect. limit	50
SLP-1	505
SLP-2	170
SLP-3	68
SLP-4	59
SLP-5	70
SLP-6	63
SLP-7	160
SLP-8	127
SLP-9	135
SLP-10	79
SLP-11	149
SLP-11R	136
SLP-12	216
SLP-13	90
SLP-14	89
SLP-15	108
SLP-16	103
SLP-17	61